

Interaction Notes

Note 425

October 1981

Frequency-Domain Response of the E-4B
Trailing-Wire Antenna

by

F.C. Yang

V. Tatoian

L. Marin

The Dikewood Corp.
Santa Monica, California

Abstract

The frequency variation of the current induced by a time-harmonic plane wave on the trailing-wire antenna on the E-4B is calculated. The calculations are based on a model of the aircraft consisting of a set of intersecting sticks with the attached antenna wires. The current on the aircraft is expanded in a set of standing waves using an asymptotic antenna theory due to Hallen. The current on the antenna wires is expanded in a set of traveling waves using an asymptotic antenna theory due to Shen et al. and refined by Chang et al. to cover all directions of propagation of the incident field. Results for the frequency variation of the induced current for many angles of incidence are presented. The important excitation mechanisms for the antenna wire currents are also discussed.

PREFACE

We wish to thank Drs. M.G. Harrison, J.P. Castillo, C.E. Baum of the Air Force Weapons Laboratory and Dr. K.S.H. Lee of the Dikewood Corporation for many enlightning discussions.

CONTENTS

<u>Section</u>	<u>Page</u>
I INTRODUCTION	8
II FORMULATION	16
III RESULTS FOR WIRE CURRENTS	22
IV COMPARISON WITH EXISTING RESULTS	38
V COMPARISON OF WIRE RESPONSES TO DIFFERENT EXCITATION MECHANISMS	43
VI CONCLUSIONS	58
APPENDIX A	59
REFERENCES	62

ILLUSTRATIONS

<u>Figure</u>		<u>Page</u>
1	The E-4B with an extended trailing-wire antenna exposed to an incident EMP.	10
2	Summary of existing TWA analysis.	11
3	Approach and assumptions used in the Boeing analysis of the E-4B trailing-wire antenna.	12
4	Approach and assumptions used in the Kaman analysis of the TACAMO trailing-wire antenna.	13
5	Approach and assumptions used in the Dikewood low frequency analysis of the E-4B trailing-wire antenna.	14
6	Approach and assumptions used in the Dikewood analysis of the E-4B trailing-wire antenna.	15
7	Decomposition of trailing-wire antenna interaction problem	17
8	Current definitions and stick model dimensions of the aircraft used in the calculations of I_{ind}^{SW} and I_{ind}^{LW} .	18
9	Magnitude of I_{SW} in the frequency ranges of 0.5-1 MHz and 1-6 MHz for $\theta = 30^\circ$.	24
10	Magnitude of I_{SW} in the frequency ranges of 0.5-1 MHz and 1-6 MHz for $\theta = 60^\circ$.	25
11	Magnitude of I_{SW} in the frequency ranges of 0.5 - 1 MHz and 1-6 MHz for $\theta = 90^\circ$.	26
12	Magnitude of I_{SW} in the frequency ranges of 0.5-1 MHz and 1-6 MHz for $\theta = 120^\circ$.	27
13	Magnitude of I_{SW} in the frequency ranges of 0.5-1 MHz and 1-6 MHz for $\theta = 150^\circ$.	28
14	Magnitude of I_{SW} in the frequency ranges of 0.5-1 MHz and 1-6 MHz for $\theta = 155^\circ$.	29

ILLUSTRATIONS (Continued)

<u>Figure</u>		<u>Page</u>
15	Magnitude of I_{SW} in the frequency ranges of 0.5-1 MHz and 1-6 MHz for $\theta = 177^\circ$.	30
16	Magnitude of I_{LW} in the frequency ranges of 0.5-1 MHz and 1-6 MHz for $\theta = 30^\circ$.	31
17	Magnitude of I_{LW} in the frequency ranges of 0.5-1 MHz and 1-6 MHz for $\theta = 60^\circ$.	32
18	Magnitude of I_{LW} in the frequency ranges of 0.5-1 MHz and 1-6 MHz for $\theta = 90^\circ$.	33
19	Magnitude of I_{LW} in the frequency ranges of 0.5-1 MHz and 1-6 MHz for $\theta = 120^\circ$.	34
20	Magnitude of I_{LW} in the frequency ranges of 0.5-1 MHz and 1-6 MHz for $\theta = 150^\circ$.	35
21	Magnitude of I_{LW} in the frequency ranges of 0.5-1 MHz and 1-6 MHz for $\theta = 155^\circ$.	36
22	Magnitude of I_{LW} in the frequency ranges of 0.5-1 MHz and 1-6 MHz for $\theta = 177^\circ$.	37
23	Comparison of the new results with the old results of $ I_{SW} $ in the frequency range of 0.5-1 MHz for $\theta = 155^\circ$.	39
24	Comparison of the new results with the old results of $ I_{SW} $ in the frequency range of 1-6 MHz for $\theta = 155^\circ$.	40
25	Comparison of the new results with the old results of $ I_{SW} $ in the frequency range of 0.5-1 MHz for $\theta = 177^\circ$.	41
26	Comparison of the new results with the old results of $ I_{SW} $ in the frequency range of 1-6 MHz for $\theta = 177^\circ$.	42
27	Decomposition of the actual excitation problem into excitation of the aircraft itself, the short antenna wire, and the long antenna wire.	45

ILLUSTRATIONS (Continued)

<u>Figure</u>		<u>Page</u>
28	Comparison of $ I_{SW} $ when both wires and the aircraft are excited with that when only the short wire and the aircraft are excited for $\theta = 30^\circ$ and $L_1 = L_2 \rightarrow \infty$.	46
29	Comparison of $ I_{SW} $ when only the aircraft is excited with that when only the wires are excited for $\theta = 30^\circ$ and $L_1 = L_2 \rightarrow \infty$.	47
30	Comparison of $ I_{LW} $ when both wires and the aircraft are excited with that when only the long wire and the aircraft are excited for $\theta = 30^\circ$ and $L_1 = L_2 \rightarrow \infty$.	48
31	Comparison of $ I_{LW} $ when only the aircraft is excited with that when only the wires are excited for $\theta = 30^\circ$ and $L_1 = L_2 \rightarrow \infty$.	49
32	Comparison of $ I_{SW} $ when both wires and the aircraft are excited with that when only the short wire and the aircraft are excited for $\theta = 155^\circ$ and $L_1 = L_2 \rightarrow \infty$.	50
33	Comparison of $ I_{SW} $ when only the aircraft is excited with that when only the wires are excited for $\theta = 155^\circ$ and $L_1 = L_2 \rightarrow \infty$.	51
34	Comparison of $ I_{LW} $ when both wires and the aircraft are excited with that when only the long wire and the aircraft are excited for $\theta = 155^\circ$ and $L_1 = L_2 \rightarrow \infty$.	52
35	Comparison of $ I_{LW} $ when only the aircraft is excited with that when only the wires are excited for $\theta = 155^\circ$ and $L_1 = L_2 \rightarrow \infty$.	53
36	Comparison of $ I_{SW} $ when both wires and the aircraft are excited with that when only the short wire and the aircraft are excited for $\theta = 177^\circ$ and $L_1 = L_2 \rightarrow \infty$.	54
37	Comparison of $ I_{SW} $ when only the aircraft is excited with that when only the wires are excited for $\theta = 177^\circ$ and $L_1 = L_2 \rightarrow \infty$.	55

ILLUSTRATIONS (Concluded)

<u>Figure</u>		<u>Page</u>
38	Comparison of $ I_{LW} $ when both wires and the aircraft are excited with that when only the long wire and the aircraft are excited for $\theta = 177^\circ$ and L_1 and $L_2 \rightarrow \infty$.	56
39	Comparison of $ I_{LW} $ when only the aircraft is excited with that when only the wires are excited for $\theta = 177^\circ$ and L_1 and $L_2 \rightarrow \infty$.	57

SECTION I

INTRODUCTION

The EMP response of the E-4B with the VLF/LF trailing-wire antenna (TWA) extended (see Figure 1) has been analyzed by different investigators (see References 1 through 4). In addition, the responses of the trailing-wire antennas on the TACAMO and EC-135 aircraft are analyzed in References 5 through 7. A summary of existing TWA analyses is shown in Figure 2. A description of the E-4B TWA system including the way it is fed is presented in Reference 1.

The approach used in Reference 4 is based on a wire grid model for the aircraft and a transmission line model for the antenna wires. A small part of the antenna wires close to the aircraft is included into the wire grid model. The size of the grids that make up the aircraft varies with frequency as does the point where the wire grid and transmission line models are joined together. This model is used together with linearity assumptions to determine the external interaction of the aircraft and the TWA. Numerical results for the current density on the aircraft are presented both in the frequency and time domains. A summary of the Boeing approach and assumption used in the analysis of Reference 4 is shown in Figure 3.

The approach used in Reference 5 is based on an asymptotic antenna theory first developed by King, Wu and Shen (Refs. 8 and 9) and subsequently refined by Chang et al. in Reference 10. This theory is applied to the TACAMO trailing-wire antenna under the assumptions that linearity applies, that the antenna wires are perfectly conducting, that no mutual field coupling takes place between the antenna wires and that the influence on the wire current from the aircraft can be described by an admittance Y_L . Only the latter assumption require some comments. With this assumption enforced one is immediately led to the conclusion that the current at the exit point on the short wire is of equal magnitude but opposite direction to that on the long wire. Thus, there is no net current (or charge build up) on the aircraft included in this model. Using the terminology of Reference 11 this same fact can be expressed in the following way: the model used in Reference 5 incorporates the differential

current mode only, it does not include the common mode. A summary of the Kaman approach and assumptions used in the analysis of Reference 5 is shown in Figure 4.

The approach used in Reference 1 for the E-4B trailing-wire antenna is based on the Hallén asymptotic antenna theory and assuming that the aircraft is electrically small. This latter assumption limits the validity of the obtained results to below 0.5 MHz. The field interaction between the wires is included by using a superposition procedure whereby the wire currents are separated into a transmission line type current and an antenna proper type current much in the same way one does for the folded dipole. The analysis results in an equivalent circuit for the antenna wires as shown in Figure 5.

The approach used in Reference 2 is similar to the Kaman approach. It differs from the Kaman approach at two points: it employs the simpler and less accurate asymptotic antenna theory of References 8 and 9, and it incorporates the aircraft by way of a stick model. Thus, both the common mode and differential mode currents are included in the model. The asymptotic antenna theory used in Reference 2 breaks down for near grazing angles of incidence with respect to the antenna wires. Using the angle θ of Figure 6 this means that the results are not valid when θ is around 0° and 180° . In fact the model predicts an infinite current for $\theta = 180^\circ$ instead of the correct value. The purpose of this report is to incorporate the more accurate asymptotic antenna theory of Reference 10 for the antenna wire currents into the stick model used for the aircraft. In this way we obtain results that are valid for near grazing angles of incidence.

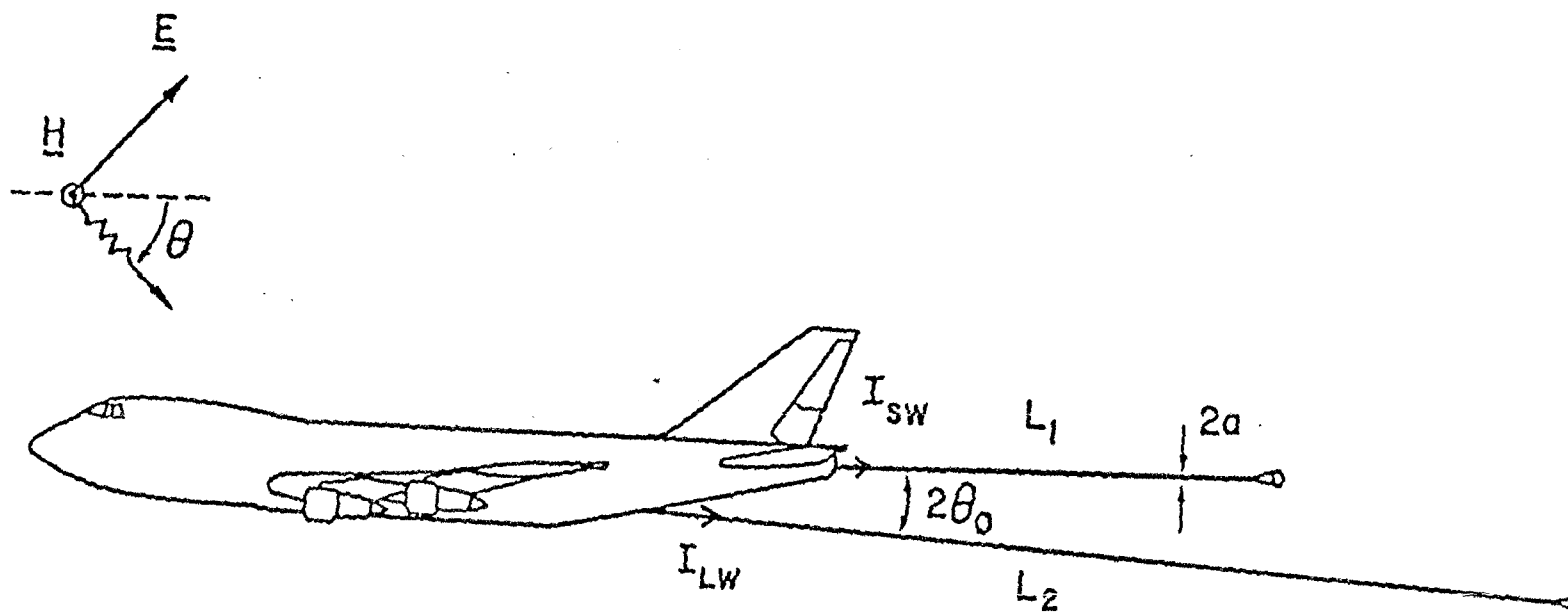


Figure 1. The E-4B with an extended trailing-wire antenna exposed to an incident EMP.

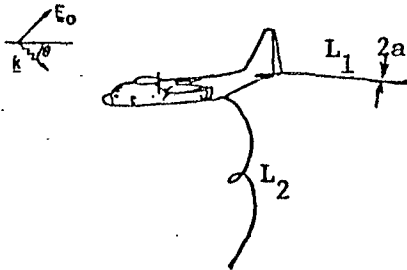
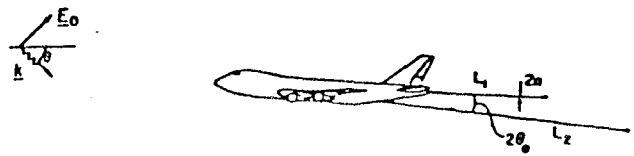
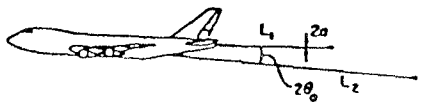
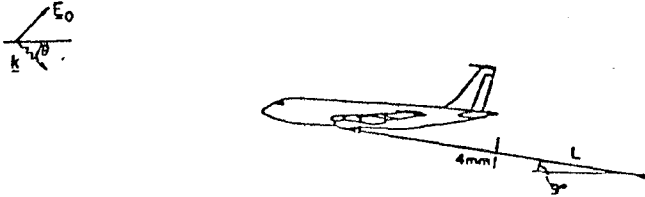
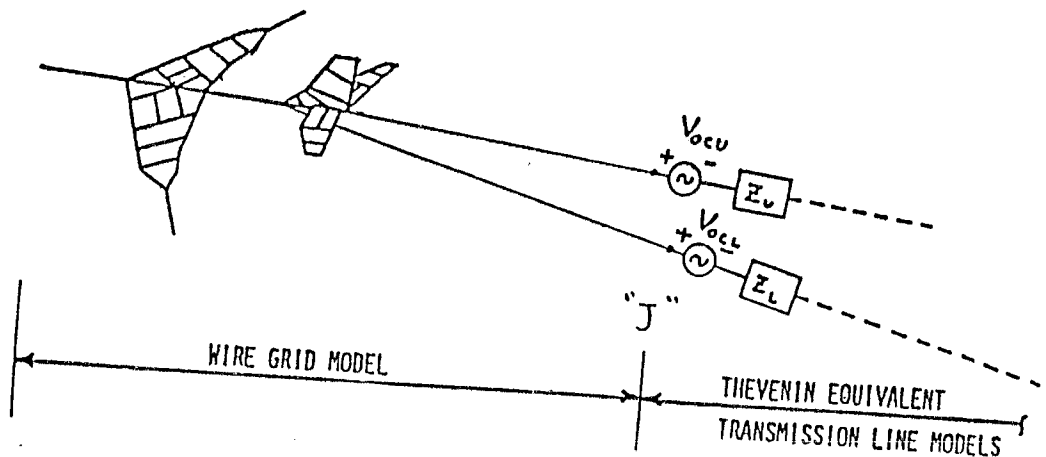
REPORT #	PREPARER	AIRCRAFT	CONFIGURATION
1	KSC	TACAMO	 <p> $a = 2 \text{ mm}$ $L_1 = 1.5 \text{ km}$ $L_2 = 9.1 \text{ km}$ </p>
2	BAC	E-4	<p> $0.3 \text{ km} < L_1 < 1.2 \text{ km}, 1.9 \text{ km} < L_2 < 8.4 \text{ km}, a = 2 \text{ mm}, \theta_0 = 3^\circ$ </p> 
3	DW	E-4 & EC-135	<p> $0.4 \text{ km} < L_1 < 1.4 \text{ km}, 2.4 \text{ km} < L_2 < 8.4 \text{ km}, a = 2 \text{ mm}, \theta_0 = 3^\circ$ </p>  <p> $2.5 \text{ km} < L < 8.5 \text{ km}$ </p> 

Figure 2. Summary of existing TWA analysis.

- APPROACH



- WIRANT MOMENT METHOD INCORPORATED WITH TRANSMISSION LINE THEORY
 - JUNCTION "J" AND GRID SIZES VARY WITH FREQUENCY

- ASSUMPTIONS

- LINEAR
- NO COUPLING BETWEEN DISTANT GRIDS

Figure 3. Approach and assumptions used in the Boeing analysis of the E-4B trailing-wire antenna.

- ASSUMPTIONS

- LINEAR (CORONA EFFECT NEGLECTED)
- PERFECTLY CONDUCTING ANTENNAS
- ANTENNAS CONNECTED BY Y_L
 - DIFFERENTIAL MODE ONLY
- IN ASYMPTOTIC ANTENNA APPROACH, ALSO ASSUME
 - ANTENNAS ARE STRAIGHT AND PERPENDICULAR TO EACH OTHER
 - NO MUTUAL COUPLING BETWEEN ANTENNAS

- ASYMPTOTIC ANTENNA THEORY
& SUPERPOSITION

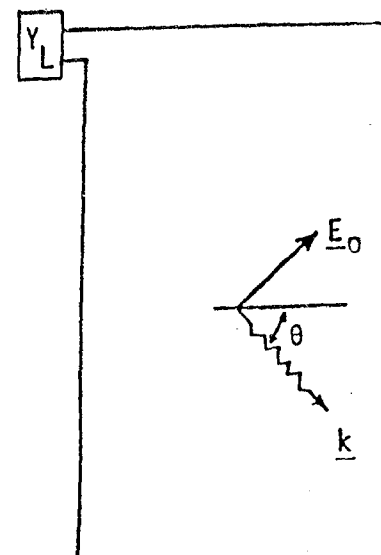


Figure 4. Approach and assumptions used in the Kaman analysis of the TACAMO trailing-wire antenna.

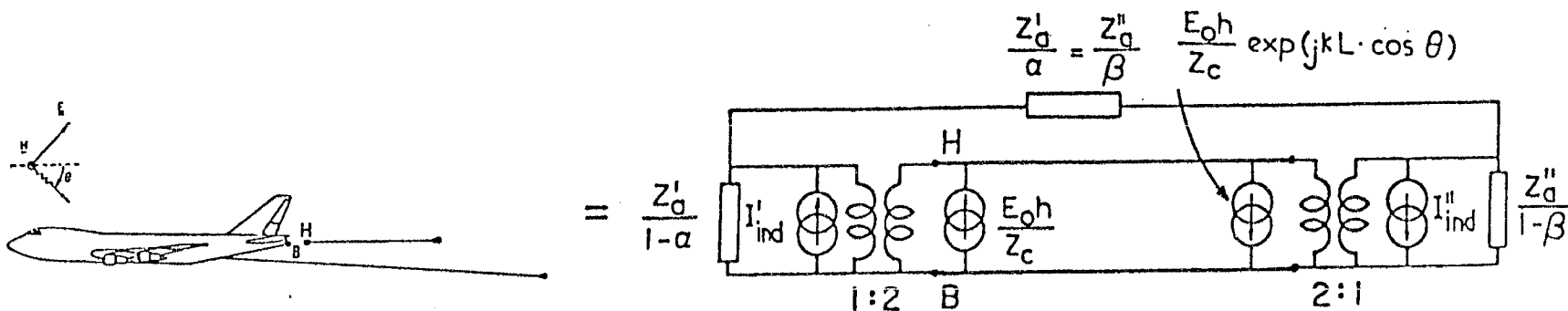
- APPROACH

- FOR FREQUENCY < 0.5 MHz

- ASYMPTOTIC ANTENNA THEORY & EQUIVALENT CIRCUIT

- A/C MODELED BY CAPACITANCE

14



- ASSUMPTIONS

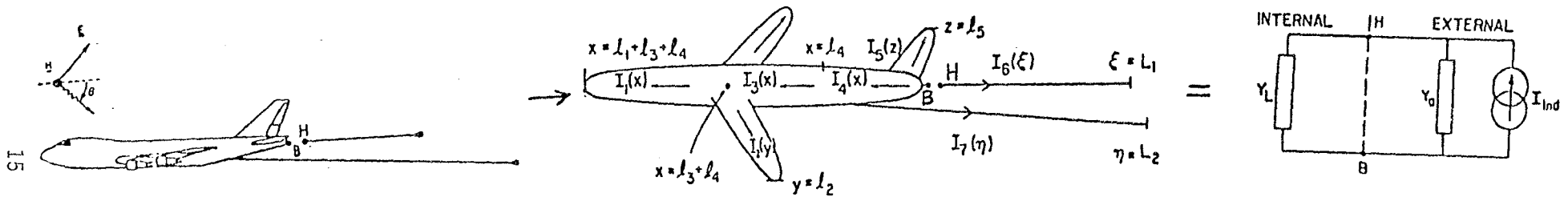
- LINEAR (CORONA EFFECT NEGLECTED)

- PERFECTLY CONDUCTING ANTENNAS

Figure 5. Approach and assumptions used in the Dikewood low frequency analysis of the E-4B trailing-wire antenna.

- APPROACH

- FOR $0.5 \text{ MHz} < \text{FREQUENCY} < 6 \text{ MHz}$
 - ASYMPTOTIC ANTENNA THEORY & EQUIVALENT CIRCUIT & SEM
 - A/C MODELED BY STICKS



- TIME-DOMAIN RESULTS ARE OBTAINED BY INVERSE FOURIER TRANSFORM
- ASSUMPTIONS
 - LINEAR (CORONA EFFECT NEGLECTED)
 - PERFECTLY CONDUCTING ANTENNAS

Figure 6. Approach and assumptions used in the Dikewood analysis of the E-4B trailing-wire antenna.

SECTION II
FORMULATION

When the antenna system is used to transmit signals, the short wire is driven against the aircraft fuselage. The long wire is grounded to the fuselage thus functioning as a counter poise. The short-wire feeding circuit has a certain impedance Z_L which can be incorporated into the model of the antenna system as shown in Figure 7a. To incorporate the effects of Z_L upon the EMP induced wire currents we use the superposition procedure of Figure 7. This procedure is outlined in Reference 1. Using the symbols of Figure 7 (which are defined in Reference 1) one has

$$\begin{aligned} I_{SW} &= I_{ind}^{SW} / (1 + Z_L Y_a) \\ I_{LW} &= I_{ind}^{LW} - I_{ind}^{SW} Z_L Y_T (1 + Z_L Y_a) \end{aligned} \quad (1)$$

The main thrust of this report is to derive expressions for I_{ind}^{SW} and I_{ind}^{LW} based upon the theory of Reference 10.

To calculate I_{ind}^{SW} and I_{ind}^{LW} we consider the problem depicted in Figure 8 where both wires are short circuited to the aircraft. Following the approaches of References 2 and 10 we can represent the induced currents in the following manner

$$\begin{aligned} I_1(x) &= A \sin [k(x - \ell_1 - \ell_3 - \ell_4)] + I_0(x, \theta) \\ &\quad - I_0(\ell_1 + \ell_3 + \ell_4, \theta) \cos [k(x - \ell_1 - \ell_3 - \ell_4)], \quad \ell_3 + \ell_4 \leq x \leq \ell_1 + \ell_3 + \ell_4 \\ I_2(y) &= B \sin [k(y - \ell_2)], \quad 0 \leq y \leq \ell_2 \\ I_3(x) &= C \sin [k(x - \ell_4)] + D \cos [k(x - \ell_4)] + I_0(x, \theta), \quad \ell_4 \leq x \leq \ell_3 + \ell_4 \\ I_4(x) &= E \sin [k(x - \ell_4)] + G \cos [k(x - \ell_4)] + I_0(x, \theta), \quad 0 \leq x \leq \ell_4 \end{aligned} \quad (2)$$

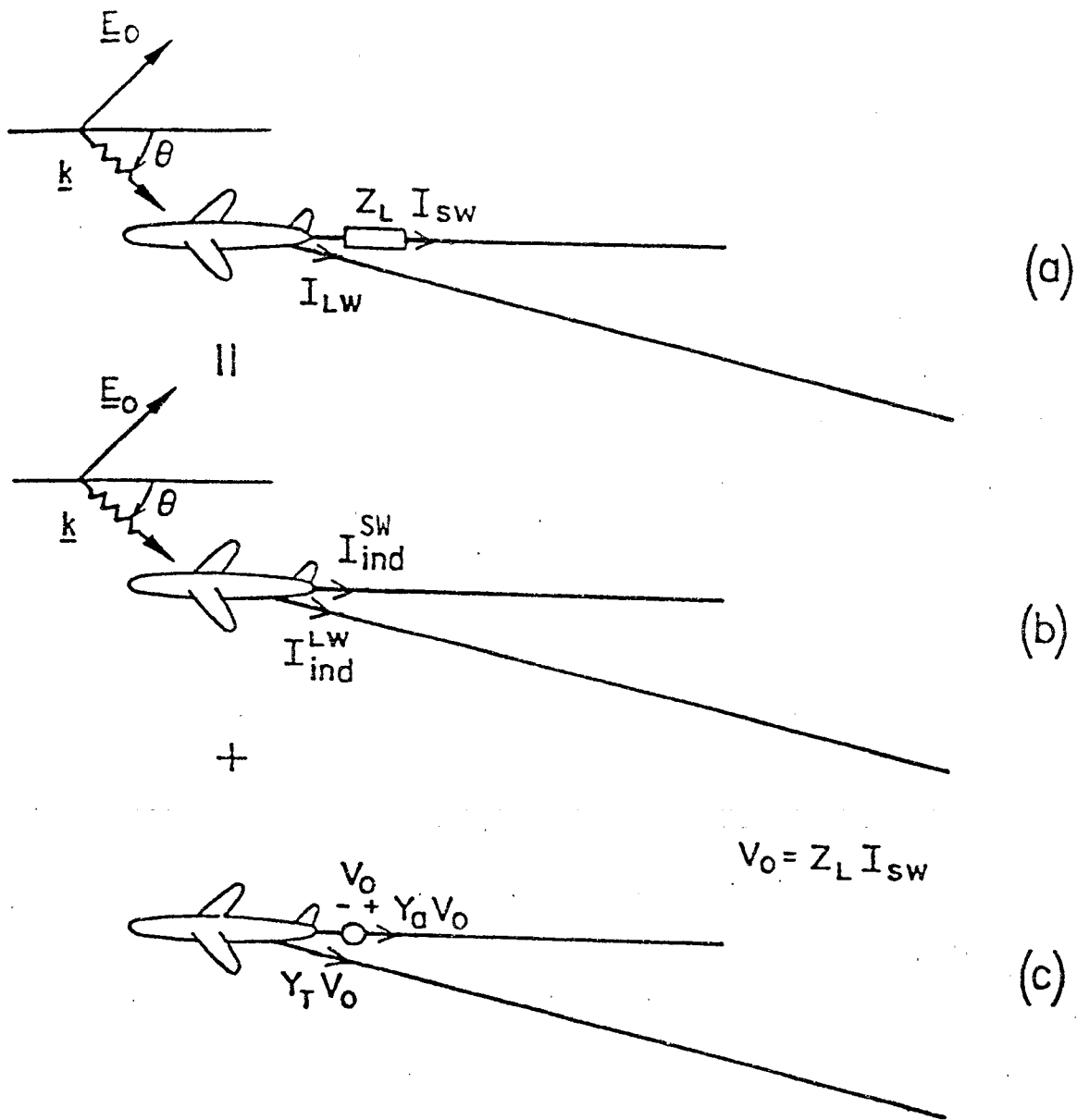
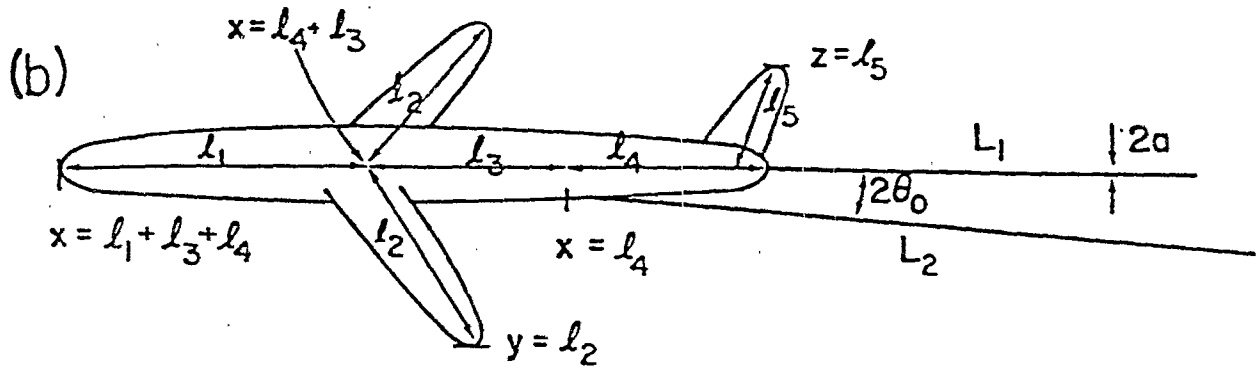
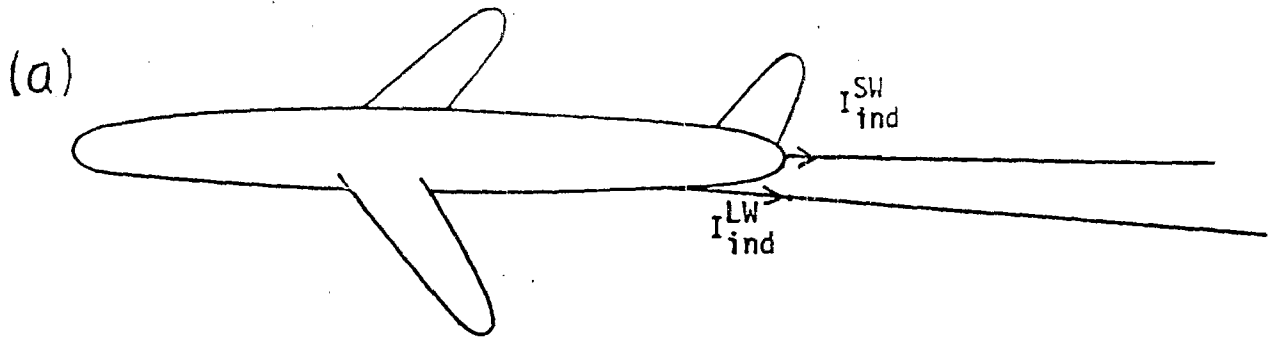


Figure 7. Decomposition of trailing-wire antenna interaction problem.



$$l_1 = 25\text{m}, l_2 = 36\text{m}, l_3 = 24\text{m}, l_4 = 12\text{m}, l_5 = 16\text{m}$$

$$L_1 = 1.2\text{km}, L_2 = 7.2\text{km}, a = 2\text{mm}, \Omega = 6.2, \theta_0 = 3^\circ$$

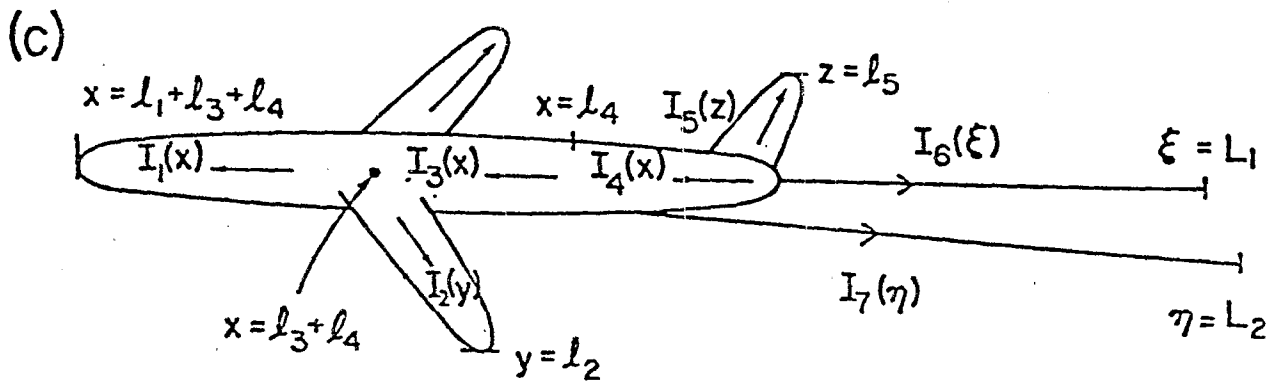


Figure 8. Current definitions and stick model dimensions of the aircraft used in the calculations of I_{ind}^{SW} and I_{ind}^{LW} .

$$I_5(z) = H \sin [k(z - \ell_5)] - I_0\left(z, \frac{\pi}{2} - \theta\right) + I_0\left(\ell_5, \frac{\pi}{2} - \theta\right) \cos [k(z - \ell_5)]$$

$$0 \leq z \leq \ell_5$$

$$I_6(\xi) = I_S(\xi, \theta) - I_S(L_1, \theta) R(\pi - \theta, L_1 - \xi) F(L_1 - \xi)$$

$$+ K \left[F(\xi) - F(L_1) R(\pi, L_1 - \xi) F(L_1 - \xi) \right]$$

$$0 \leq \xi \leq L_1$$

$$I_7(\eta) = \left[I_S(\eta, \phi) - I_S(L_2, \phi) R(\pi - \phi, L_2 - \eta) F(L_2 - \eta) \right] \exp(jk\ell_4 \cos\theta)$$

$$+ M \left[F(\eta) - F(L_2) R(\pi, L_2 - \eta) F(L_2 - \eta) \right]$$

$$0 \leq \eta \leq L_2$$

where

$$I_0(x, \theta) = \frac{E_0 \lambda}{Z_0} \frac{2j \exp(jkx \cos\theta)}{\Omega \sin\theta}$$

$$I_S(x, \theta) = \frac{E_0 \lambda}{Z_0} \frac{j \exp(-jkx \cos\theta)}{\sin\theta \left\{ \ln \left[\frac{(ka/2) \sin\theta}{\Gamma} \right] + j\pi/2 \right\}}$$

$$(3)$$

$$F(\xi) = \frac{\ln \left\{ 1 - 2\pi j / \left[\ln(\Gamma k^2 a^2) - \ln \left(k\xi + \sqrt{k^2 \xi^2 + \Gamma^{-2}} \right) + j\pi/2 \right] \right\}}{\ln \left\{ 1 - 2\pi j / \left[2 \ln(\Gamma ka) + j\pi/2 \right] \right\}} e^{-jk\xi}$$

$$R(\theta, \xi) = \psi^{-1} \left[\psi - 2 \ln(\sin(\theta/2)) - \exp(jv) E_1(jv) \right]$$

and $\lambda = 2\pi/k$, $Z_0 = \sqrt{\mu_0/\epsilon_0}$, $\Gamma = 1.781$, $\Omega \approx 6.2$, $v = k\xi(1 - \cos\theta)$, $\psi = -2 \ln(\Gamma ka) - j\pi$ and $E_1(x)$ is the exponential integral of the first kind (see Reference 12).

The difference between the formulation used here and the one used in Reference 2 lies in the "reflection coefficient" $R(\theta, \xi)$. The determination of this quantity based on the formulation and solution of a Wiener-Hopf problem is the main contribution of Reference 10. In the simpler formulation used in Reference 2 this reflection coefficient is unity. In fact the value of $R(\theta, \xi)$ as obtained from Eq.3 is close to unity except for near grazing angles of incidence (θ small).

The net results of $R(\theta, \xi)$ on the induced wire currents will be discussed later in this section.

The unknown constants A, B, C, D, E, G, H, K and M are determined from the following junction conditions (see Reference 2)

$$\begin{aligned}
 I_1(\ell_3 + \ell_4) + 2 I_2(0) - I_3(\ell_3 + \ell_4) &= 0 \\
 \frac{d}{dx} I_1(\ell_3 + \ell_4) &= \frac{d}{dy} I_2(0) = \frac{d}{dx} I_3(\ell_3 + \ell_4) \\
 I_3(\ell_4) + I_7(0) - I_4(\ell_4) &= 0 \\
 \psi \frac{d}{d\eta} I_7(0) &= \Omega \frac{d}{dx} I_3(\ell_4) = \Omega \frac{d}{dx} I_4(\ell_4) \\
 I_4(0) + I_5(0) + I_6(0) &= 0 \\
 \psi \frac{d}{d\xi} I_6(0) &= \Omega \frac{d}{dx} I_4(0) = \Omega \frac{d}{dz} I_5(0)
 \end{aligned} \tag{4}$$

After some tedious but straightforward algebraic manipulations, the unknown constants are found from these conditions. The obtained expressions for the constants are complicated and unilluminating and are consequently left out. The quantities of main interest namely, the induced short-circuit current on each wire where it is connected to the aircraft can be expressed in the following form

$$\begin{aligned}
 I_{ind}^{SW} &= I_6(0) = I_s(0, \theta) - I_s(L_1, \theta) R(\pi - \theta, L_1) F_1 \\
 &\quad + K(1 - R_1 F_1^2) \\
 I_{ind}^{LW} &= I_7(0) = \left[I_s(0, \phi) - I_s(L_2, \phi) R(\pi - \phi, L_2) F_2 \right] \exp(j k \ell_4 \cos \theta) \\
 &\quad + M(1 - R_2 F_2^2)
 \end{aligned} \tag{5}$$

Expressions for K, M, F_1, F_2, R_1 , and R_2 are presented in Appendix A.

Before presenting the numerical results obtained from the derived expressions let us briefly examine the values obtained from them when the incident wave hits the aircraft/antenna-wire system from behind, i.e., when $\theta = \pi - \epsilon$, ϵ being a small angle. The term $I_s(\xi, \theta)$ has a singularity on the order of $1/(\epsilon \ln \epsilon)$ as θ approaches π . In the formulation used in Reference 2 where $R=1$ the same singularity occurs in I_{ind}^{SW} . With the more accurate expression for $R(\theta, \xi)$ one has

$$I_s(0, \pi - \epsilon) - I_s(L_1, \pi - \epsilon)R(\epsilon, L_1)F_1 \rightarrow O(\epsilon^2 \ln \epsilon)$$

as $\epsilon \rightarrow 0$. Thus, the wire current has a finite value when the wave propagates parallel to the wire.

The behavior of the wire current for different angles of incidence will be presented in the next section.

SECTION III

RESULTS FOR WIRE CURRENTS

The formulas derived in the previous section are used in this section to present the frequency variation of the wire current for different angles of incidence.

Figures 9 through 15 show the frequency variation of the short-wire current whereas Figures 16 through 22 show the frequency variation of the long-wire current. The angles of incidence for which the data are presented include $\theta = 30^\circ$, 60° , 90° , 120° , 150° , 155° , and 177° . The angle $\theta = 155^\circ$ is the direction of incidence which is expected to result in the maximum time-domain peak value of the induced current on the short wire. Similarly, $\theta = 177^\circ$ is the direction resulting in the largest time-domain peak value of the induced long-wire current.

The resonance behavior of the wire currents are clearly exhibited in the presented results. We also observe that the long wire response is dominated by the long-wire resonances whereas the short-wire response is dominated by the short-wire resonances. This result points to the fact that the coupling between the two wires is weak. This point will be elaborated on further in Section V.

Another feature of the curves is the beating patterns seen. The beating frequency of the short wire current is $c/L_1(1 - |\cos\theta|)$ and that of the long wire current is $c/L_2(1 - |\cos\phi|)$. These two frequencies can be understood as being due to interaction between two wire current waves. The first current wave is launched on the respective wire when the wavefront first hits one of its ends and the other current wave is launched when the wavefront just passes by the other end of the wire.

The effects of the load impedance Z_L on the induced wire current is very small in the considered frequency range. The results presented in Figures 9 through 15 can therefore be taken to mean both of the quantities I_{SW} and I_{ind}^{SW} . Similarly, the curves in Figures 16 through 22 represent both I_{LW} and I_{ind}^{LW} .

All the results presented in this report are time harmonic ones. This means that Figures 9 through 22 show the responses of the antenna wires for an incident electric field of unit amplitude and harmonic time dependence. They

can also be interpreted to mean the spectral density of the wire current response due to a delta-function incident wave of unit impulse. To obtain the spectral density of the current due to any other waveshape only requires that one multiplies the presented results with the spectrum of the given waveshape.

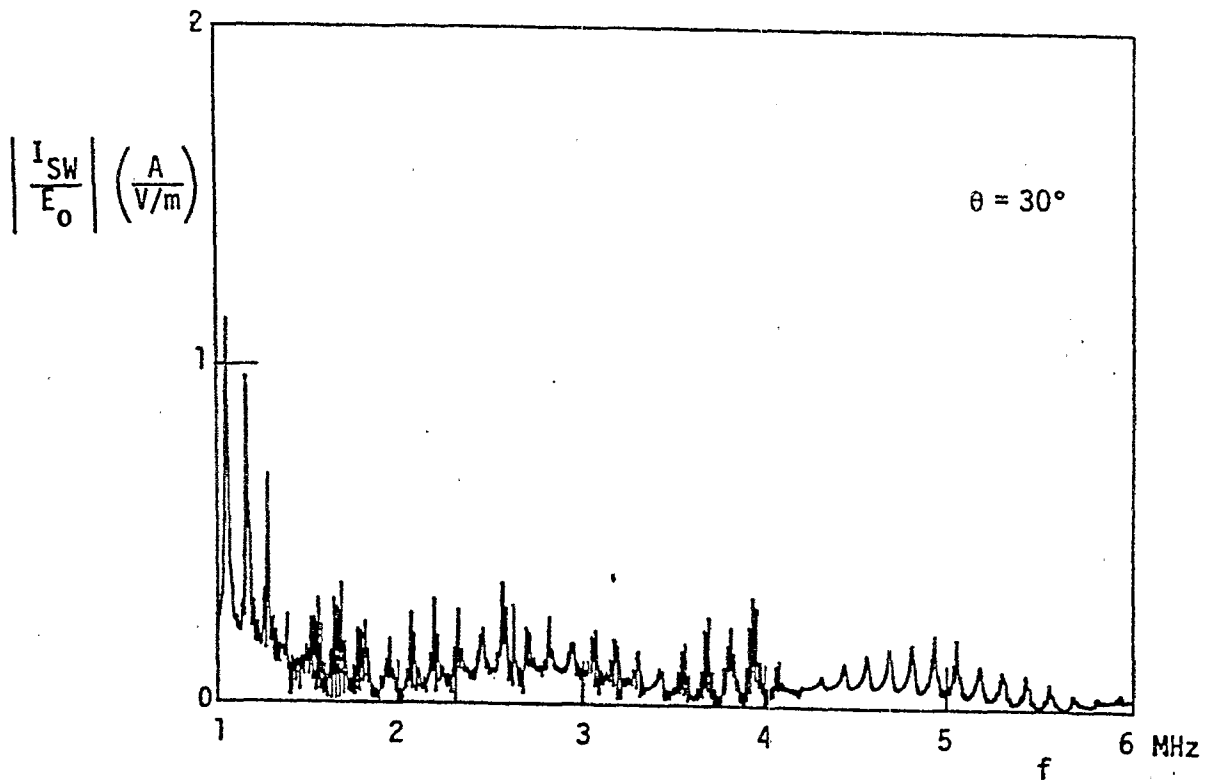
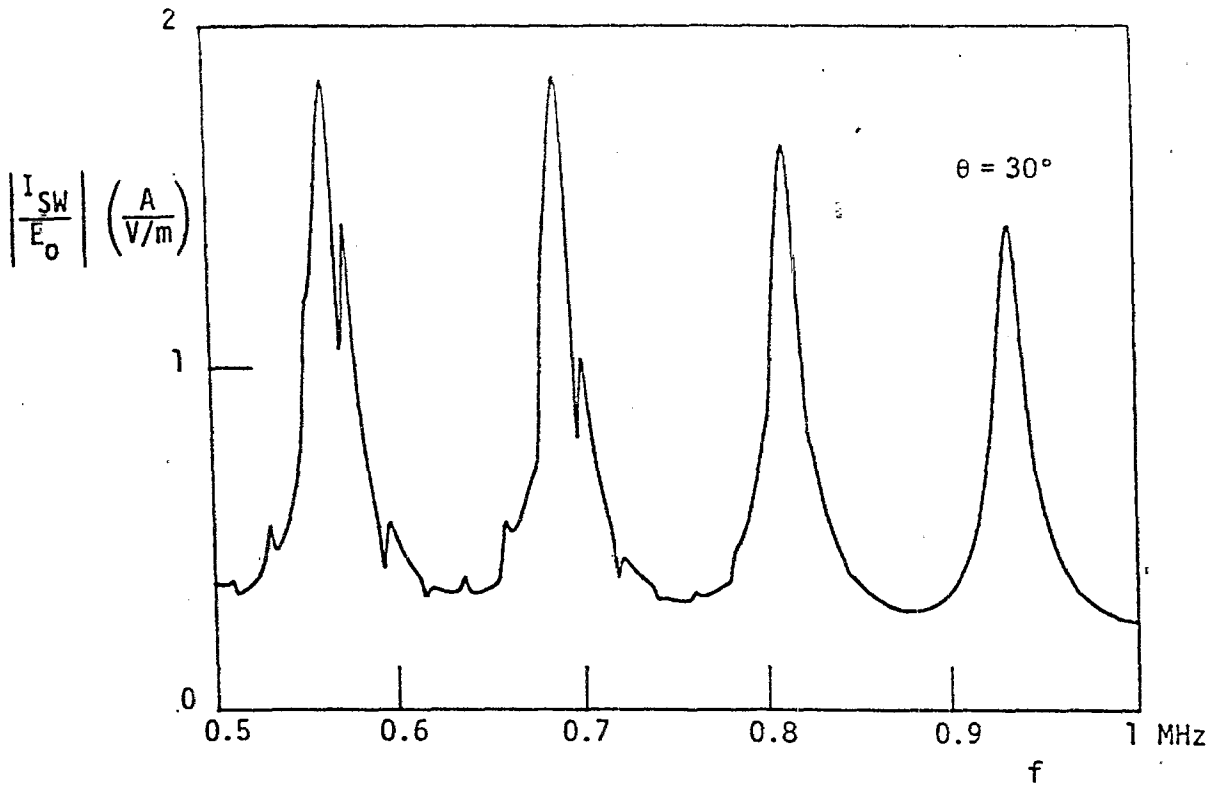


Figure 9. Magnitude of I_{SW} in the frequency ranges of 0.5-1 MHz and 1-6 MHz for $\theta=30^\circ$.

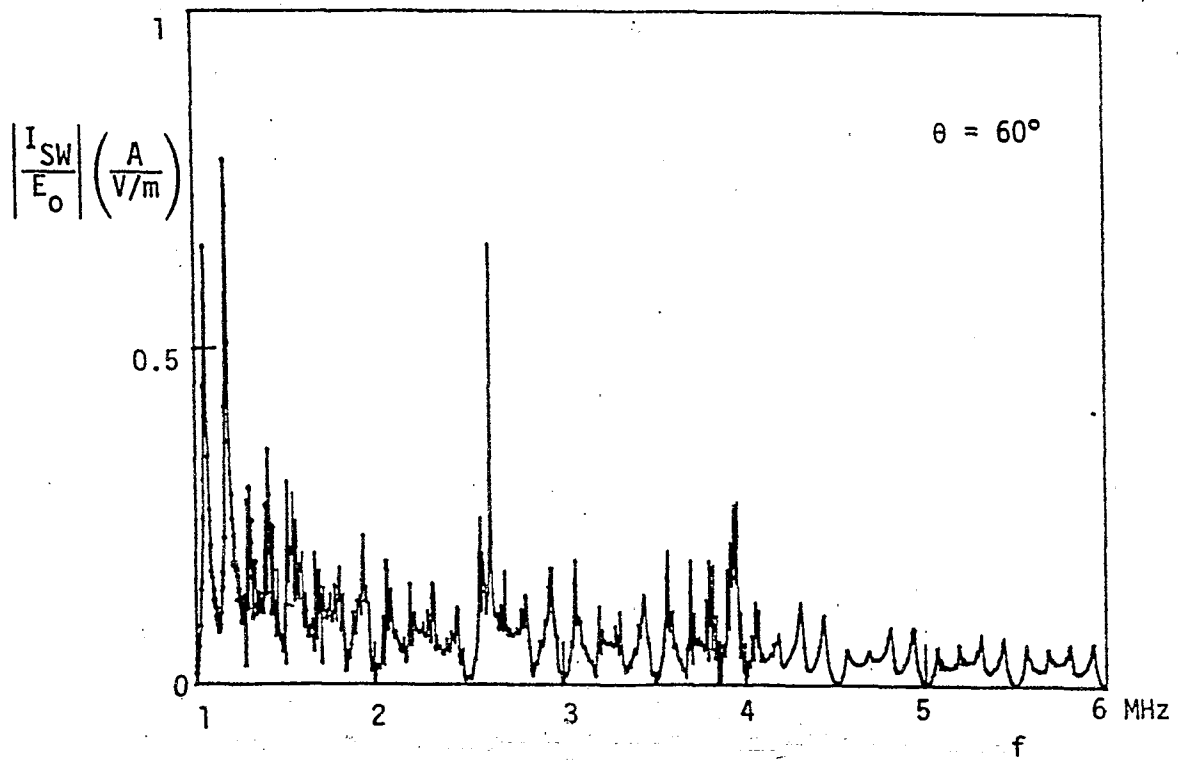
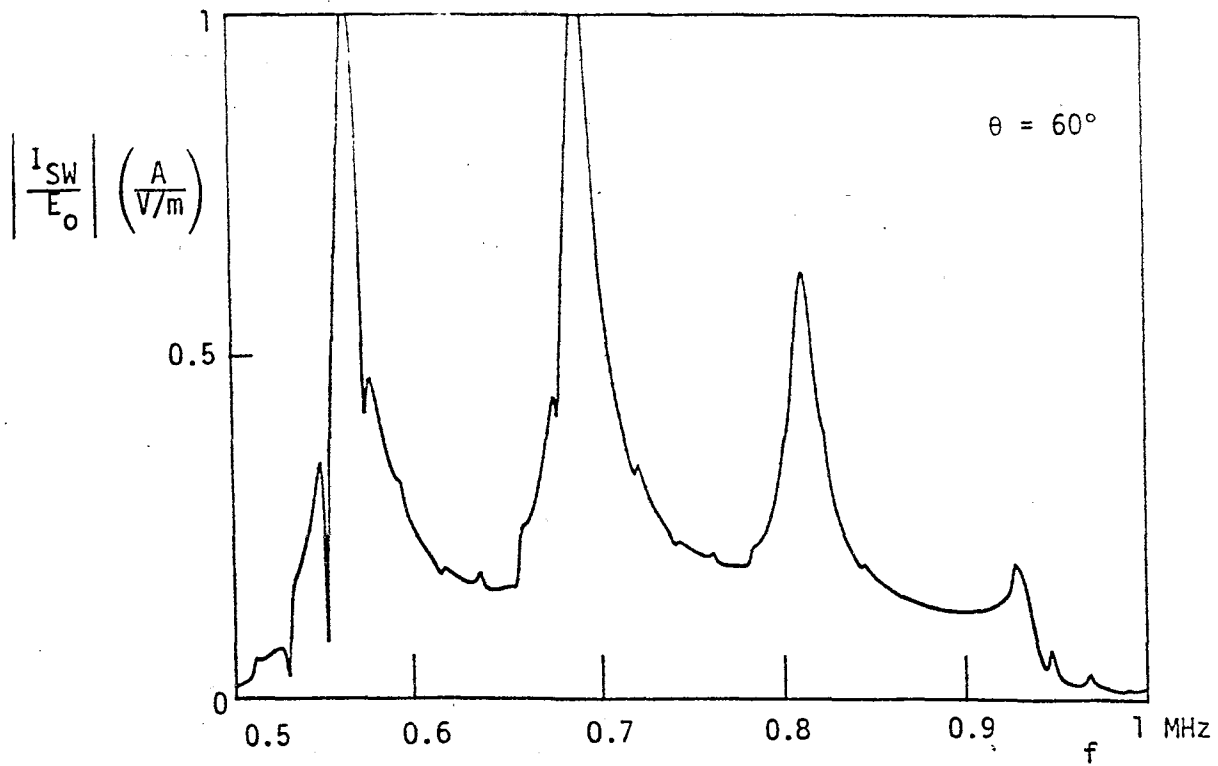


Figure 10. Magnitude of I_{SW} in the frequency ranges of 0.5-1 MHz and 1-6 MHz for $\theta=60^\circ$.

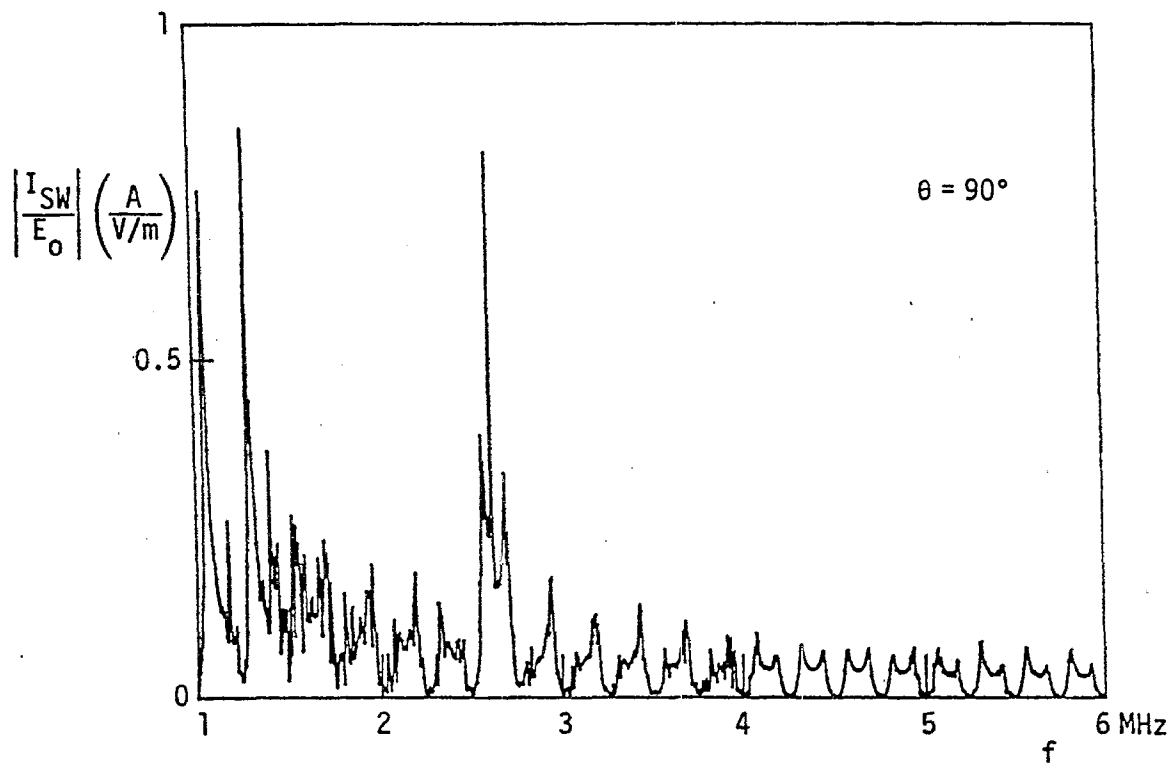
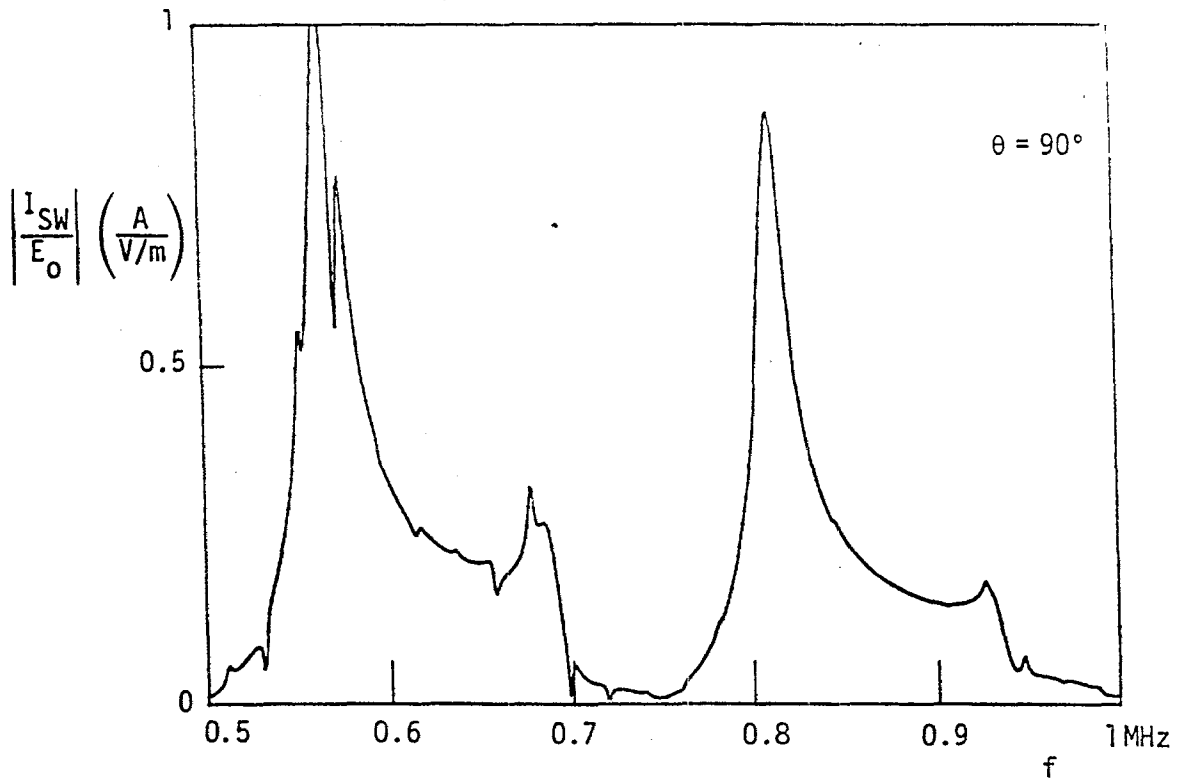


Figure 11. Magnitude of I_{SW} in the frequency ranges of 0.5-1 MHz and 1-6 MHz for $\theta = 90^\circ$.

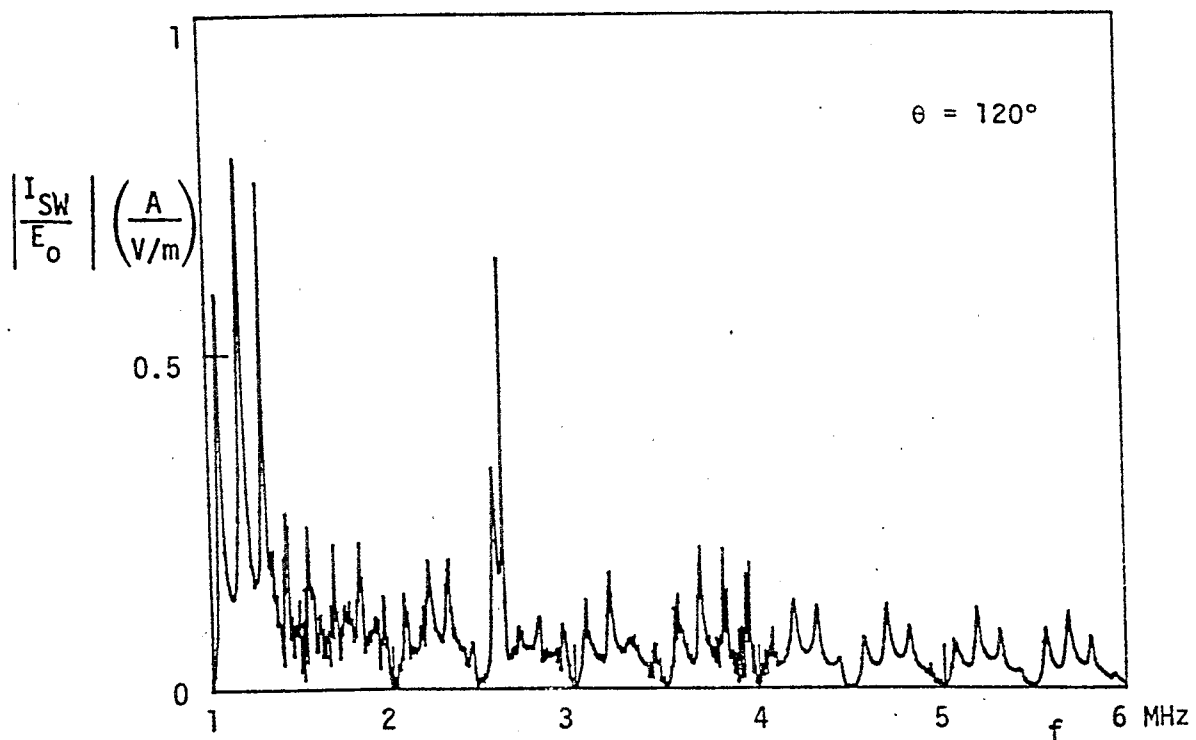
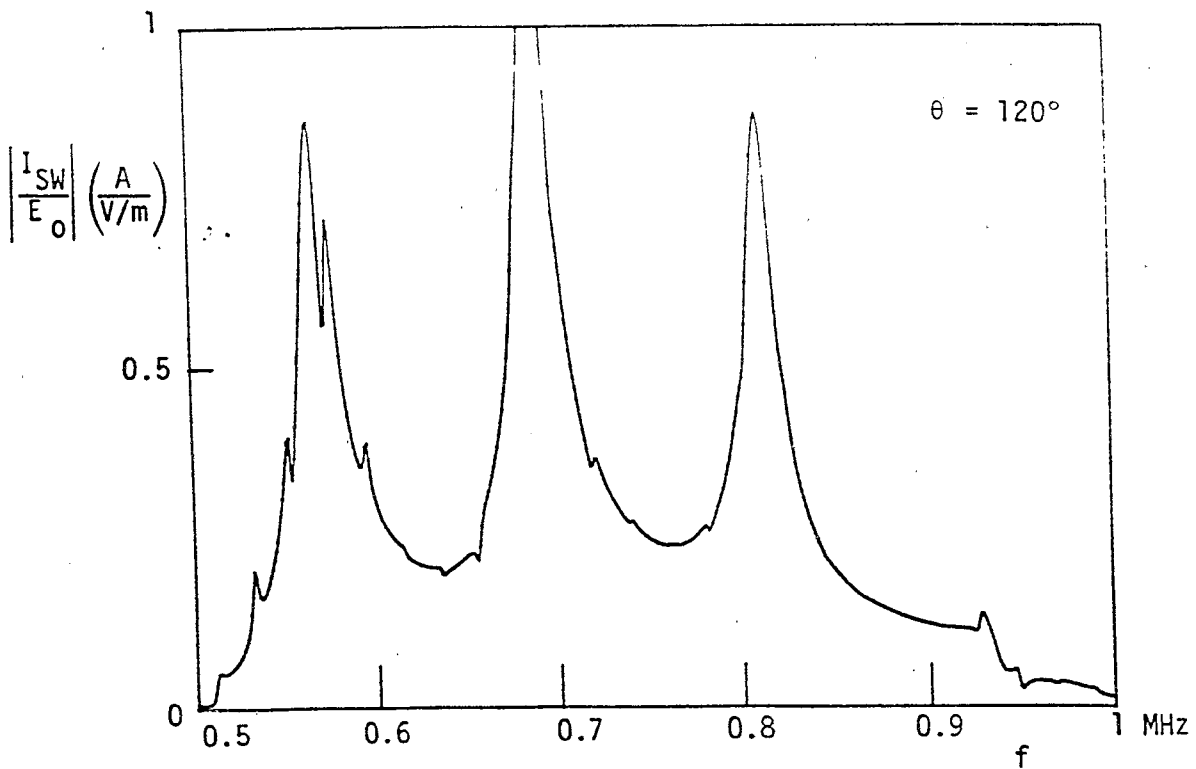


Figure 12. Magnitude of I_{SW} in the frequency ranges of 0.5-1 MHz and 1-6 MHz for $\theta=120^\circ$.

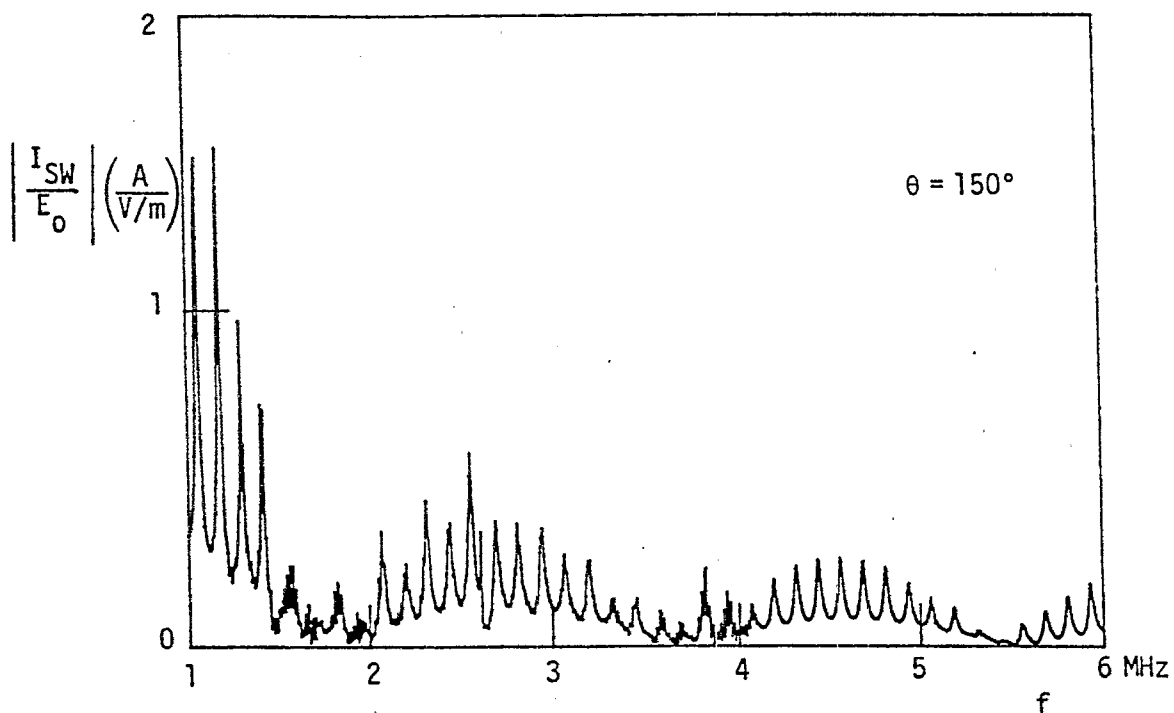
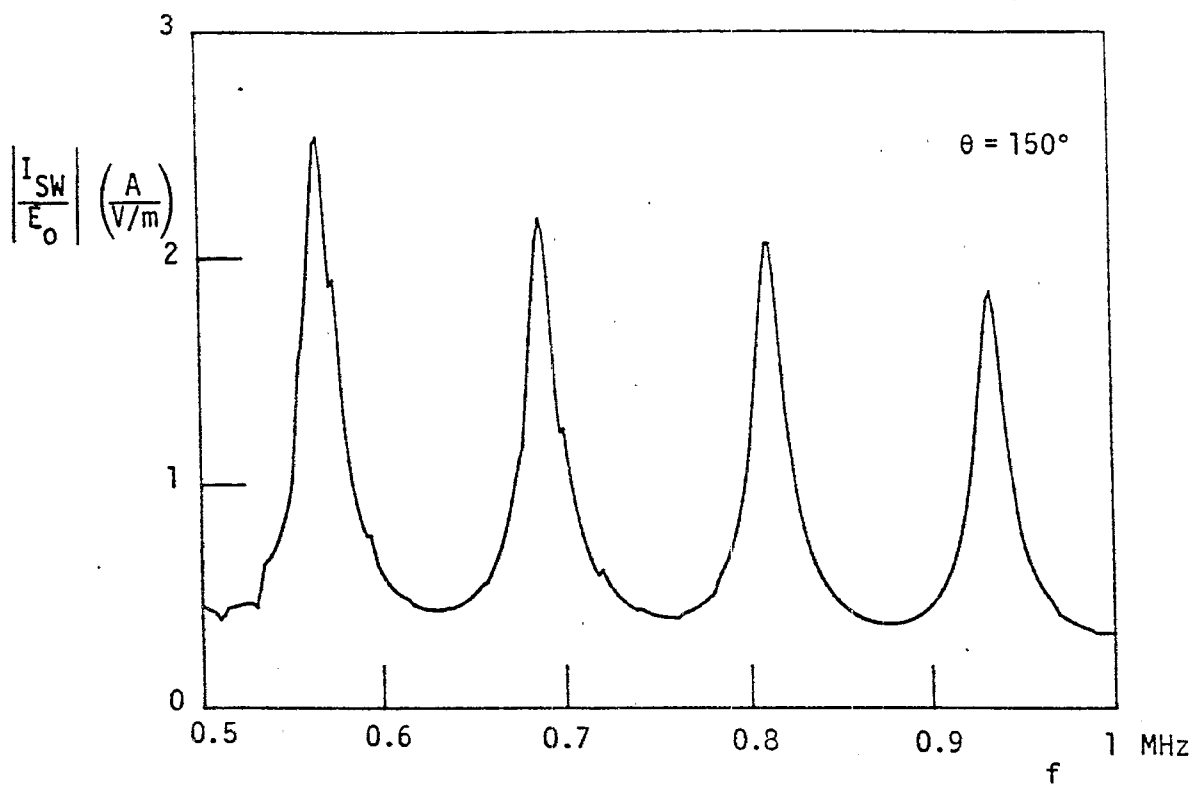
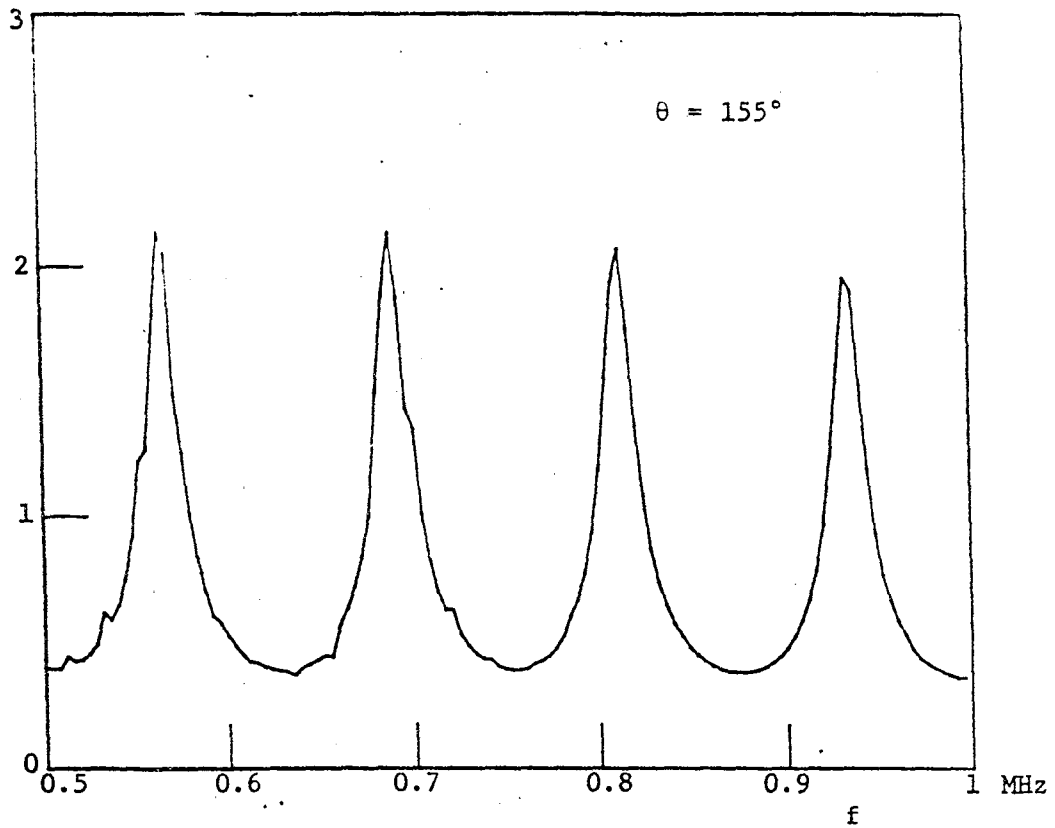


Figure 13. Magnitude of I_{SW} in the frequency ranges of 0.5-1 MHz and 1-6 MHz for $\theta = 150^\circ$.

$$\left| \frac{I_{SW}}{E_0} \right| \left(\frac{A}{V/m} \right)$$



$$\left| \frac{I_{SW}}{E_0} \right| \left(\frac{A}{V/m} \right)$$

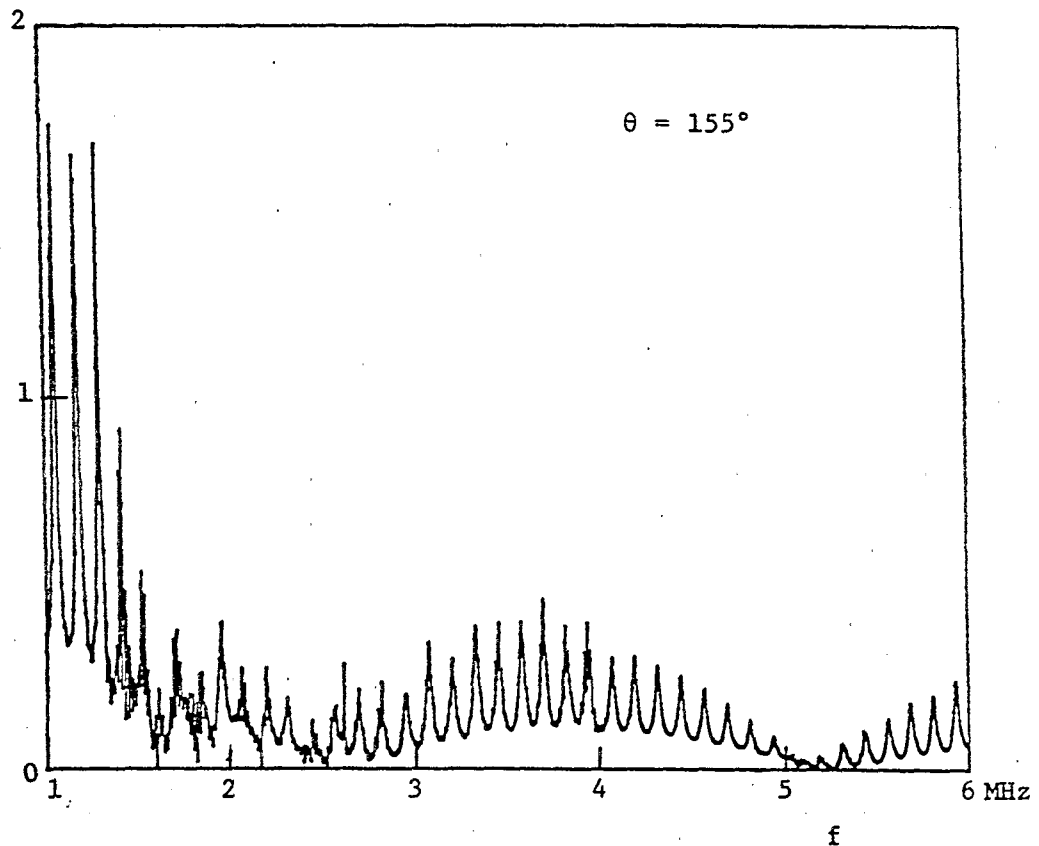
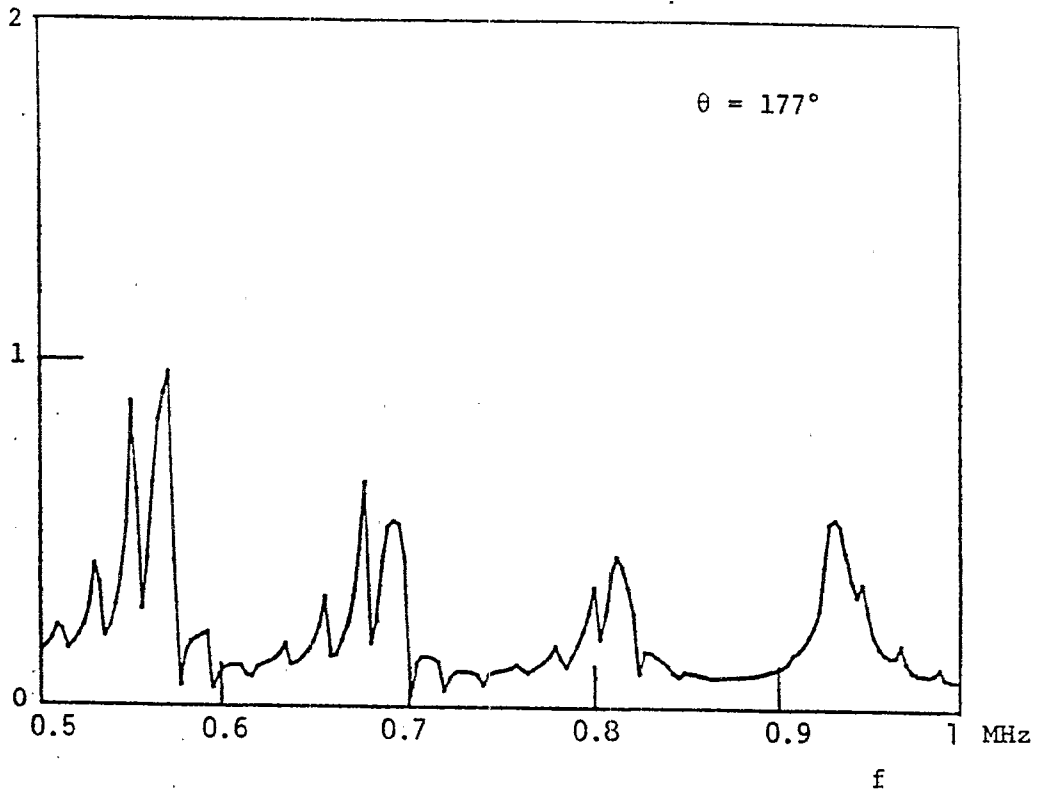


Figure 14. Magnitude of I_{SW} in the frequency ranges of 0.5-1MHz and 1-6 MHz for $\theta=155^\circ$.

$$\left| \frac{I_{SW}}{E_o} \right| \left(\frac{A}{V/m} \right)$$



$$\left| \frac{I_{SW}}{E_o} \right| \left(\frac{A}{V/m} \right)$$

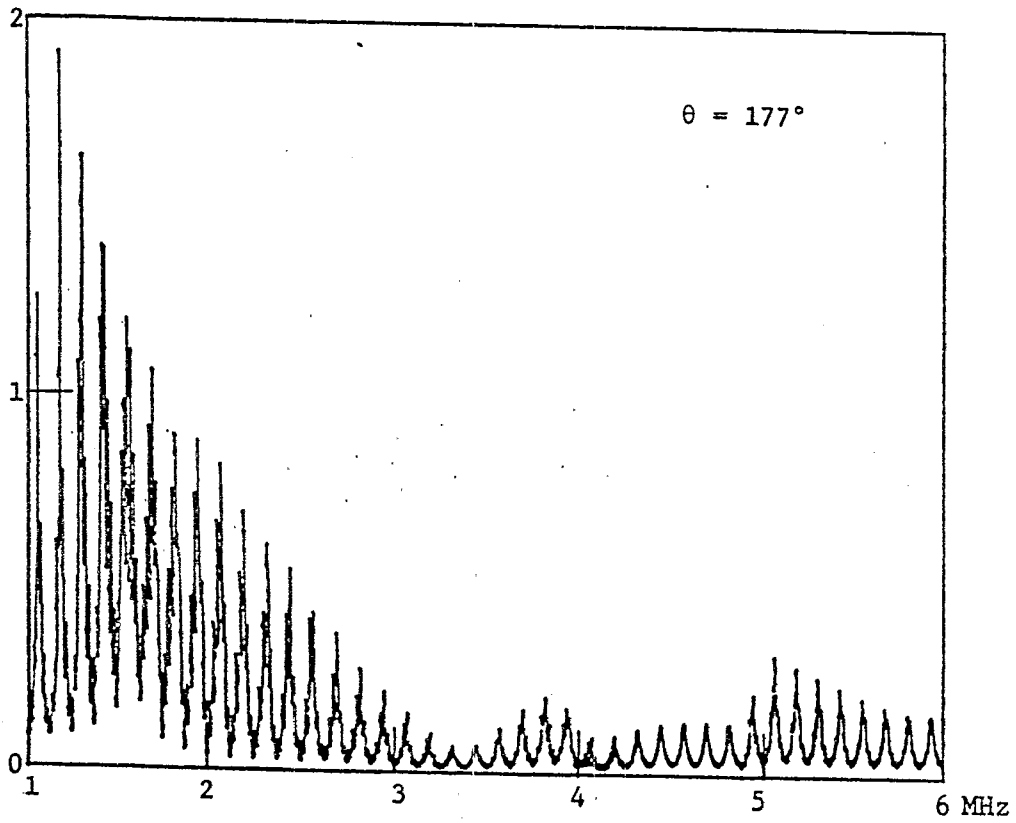


Figure 15. Magnitude of I_{SW} in the frequency ranges of $0.5-1$ MHz and $1-6$ MHz for $\theta=177^\circ$.

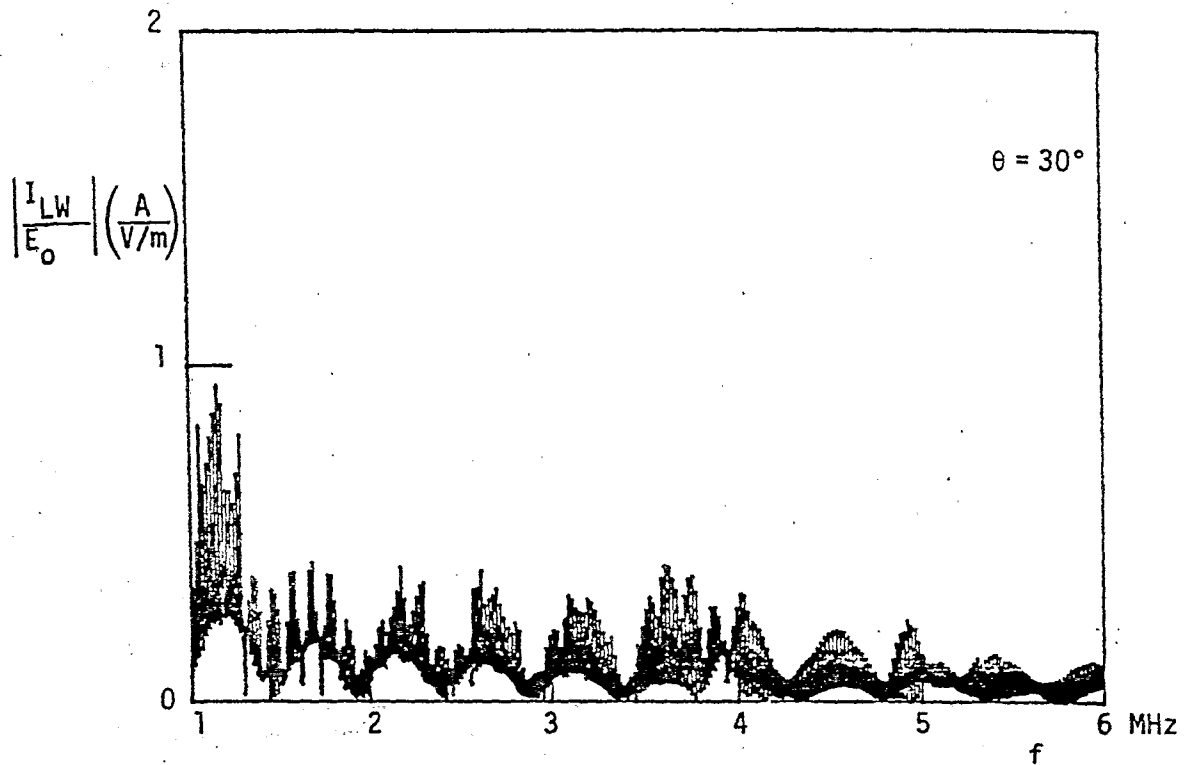
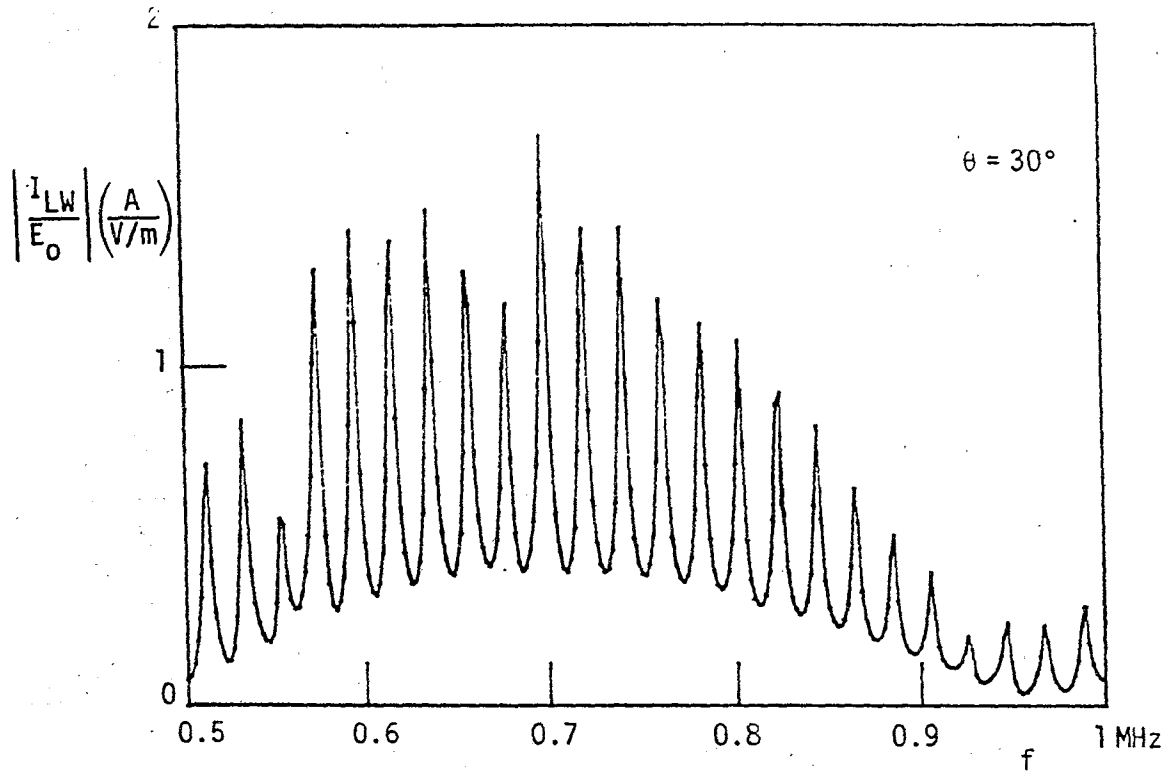


Figure 16. Magnitude of I_{LW} in the frequency ranges of 0.5-1 MHz and 1-6 MHz for $\theta = 30^\circ$.

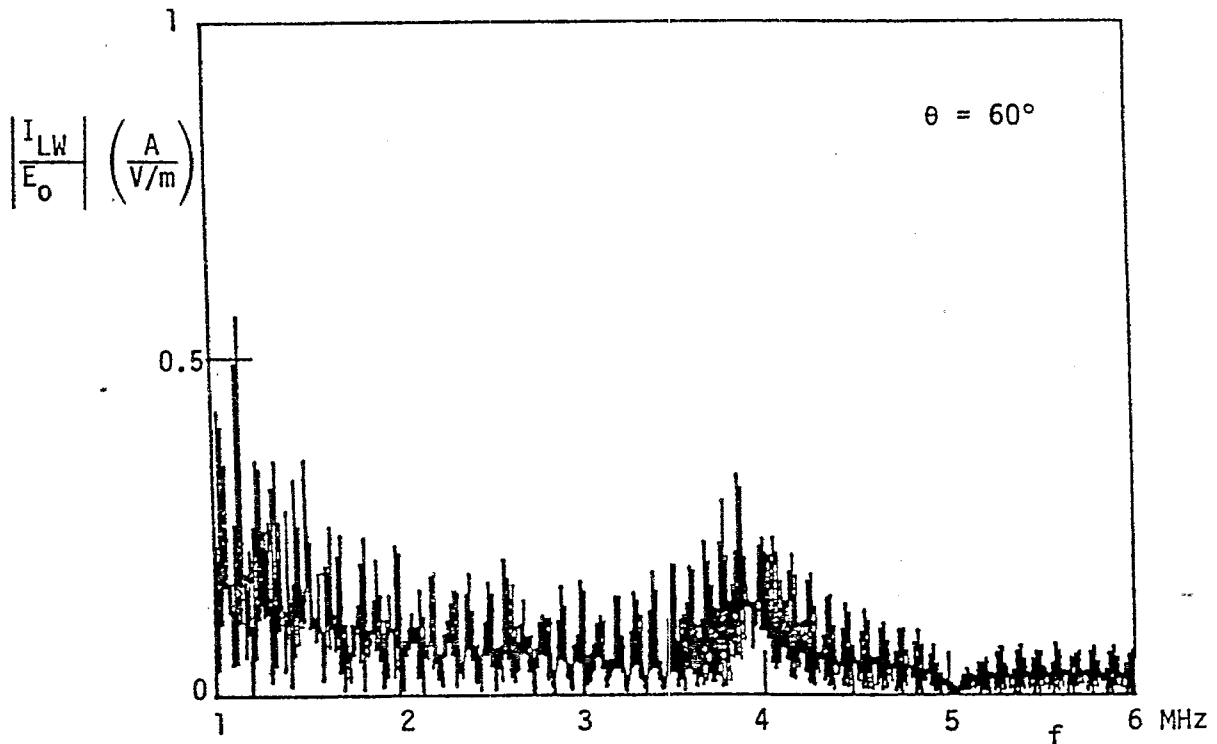
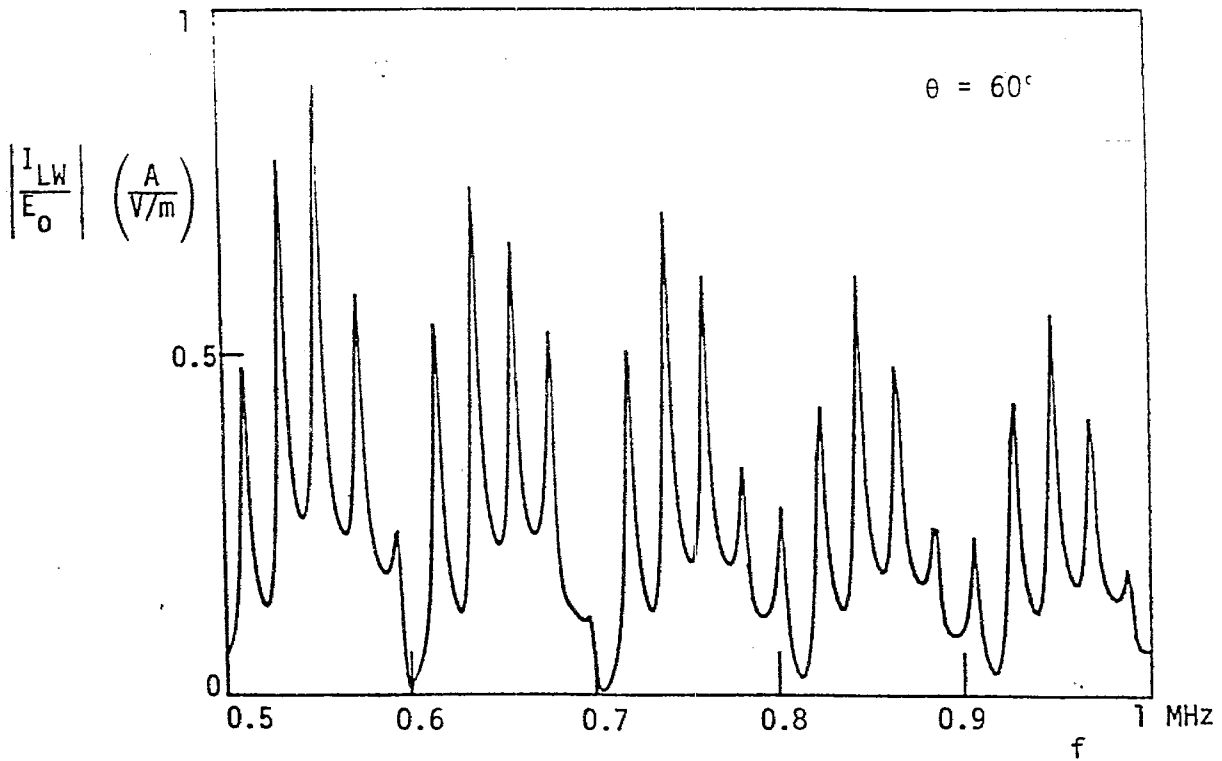


Figure 17. Magnitude of I_{LW} in the frequency ranges of 0.5-1 MHz and 1-6 MHz for $\theta=60^\circ$.

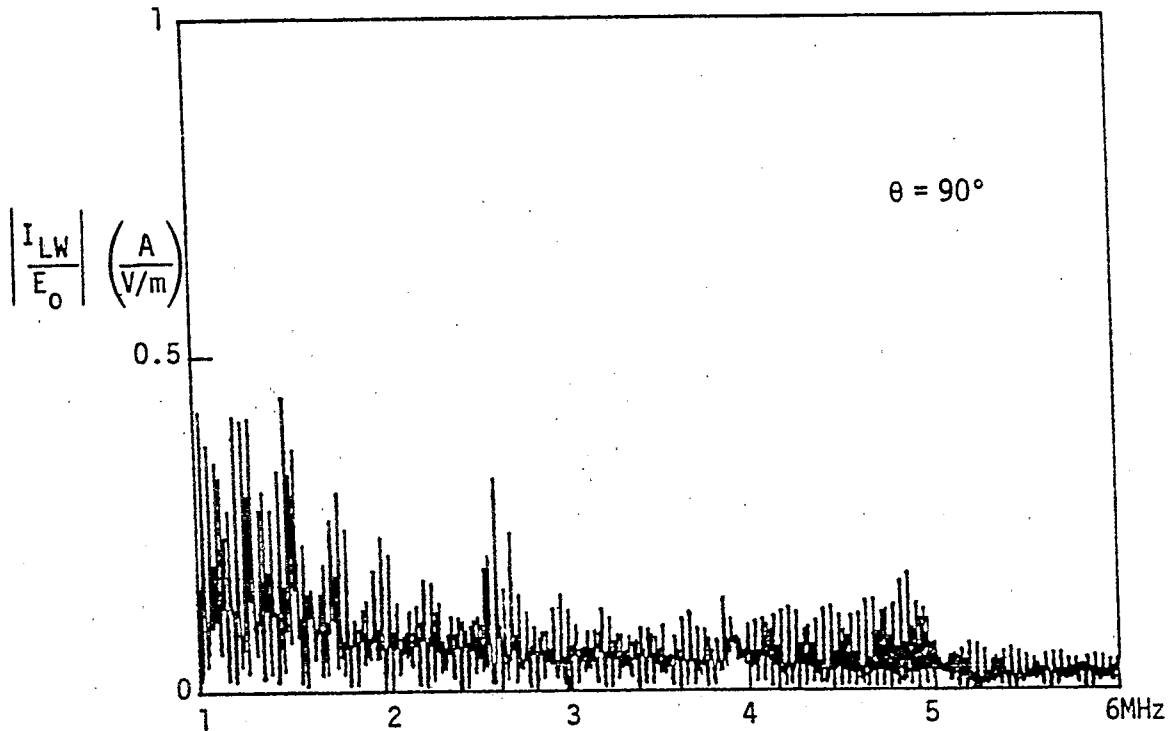
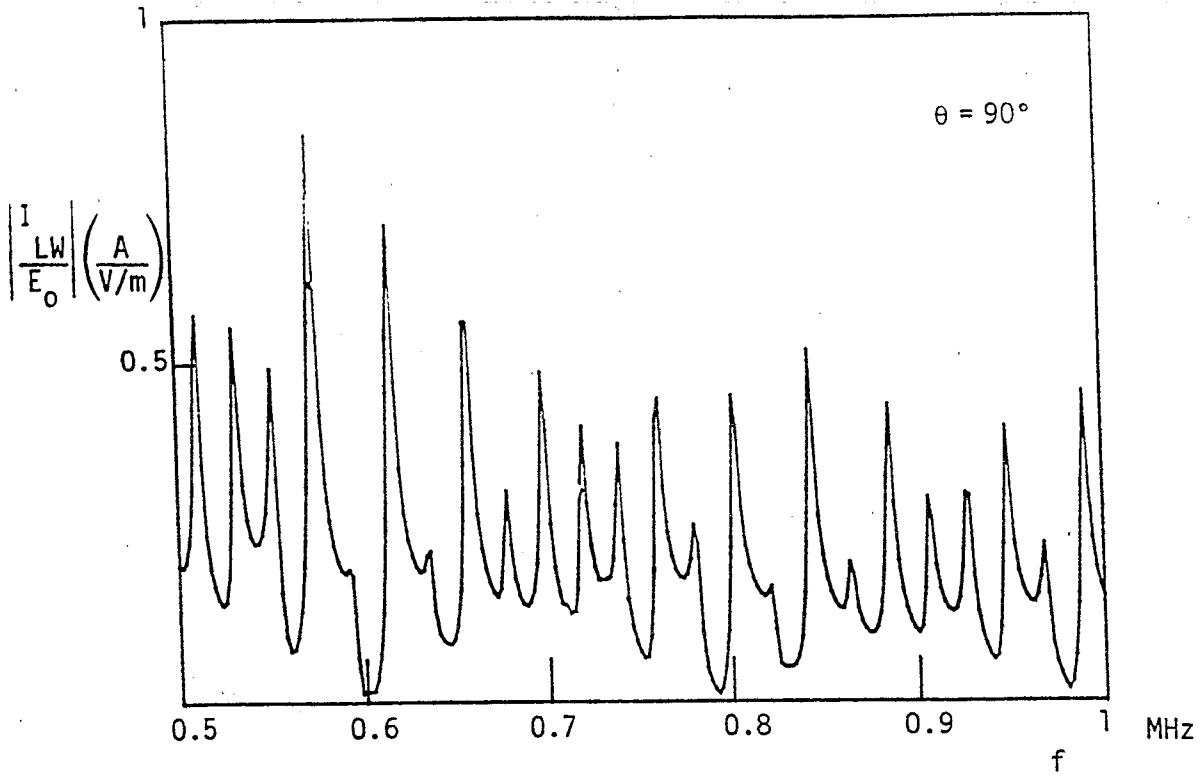


Figure 18. Magnitude of I_{LW} in the frequency ranges of 0.5-1 MHz and 1-6 MHz for $\theta = 90^\circ$.

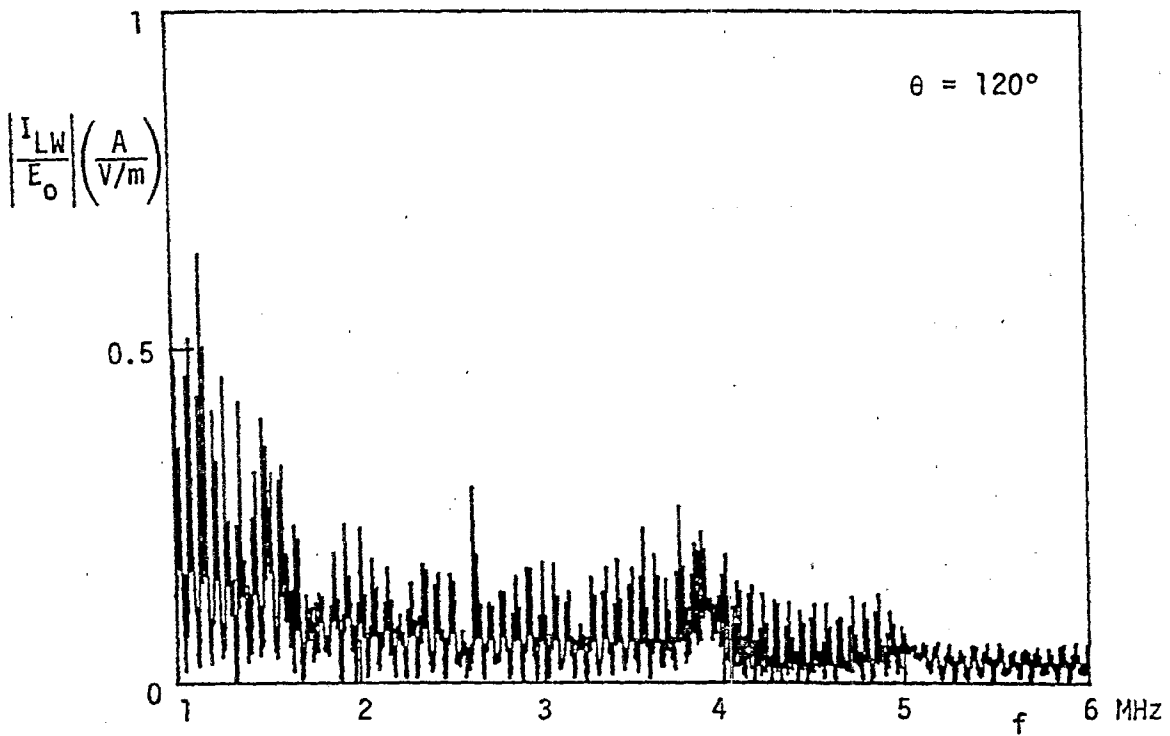
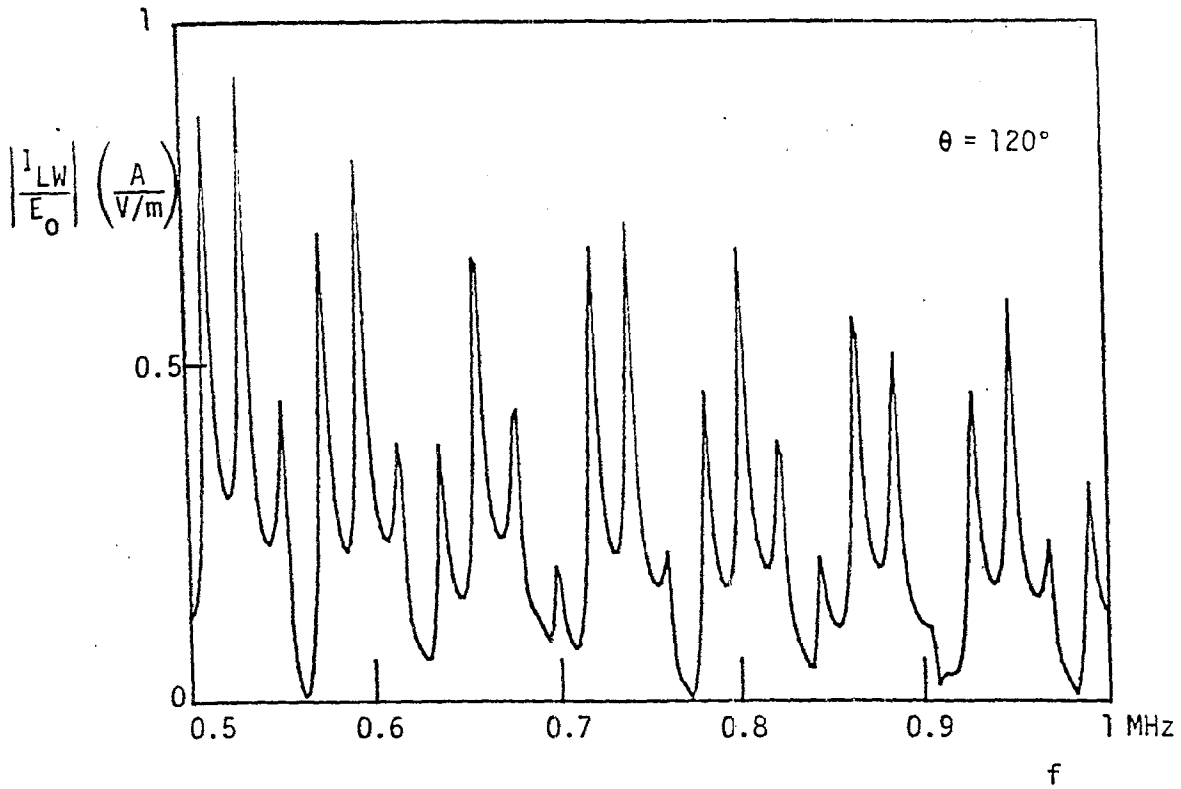


Figure 19. Magnitude of I_{LW} in the frequency ranges of 0.5-1 MHz and 1-6 MHz for $\theta = 120^\circ$.

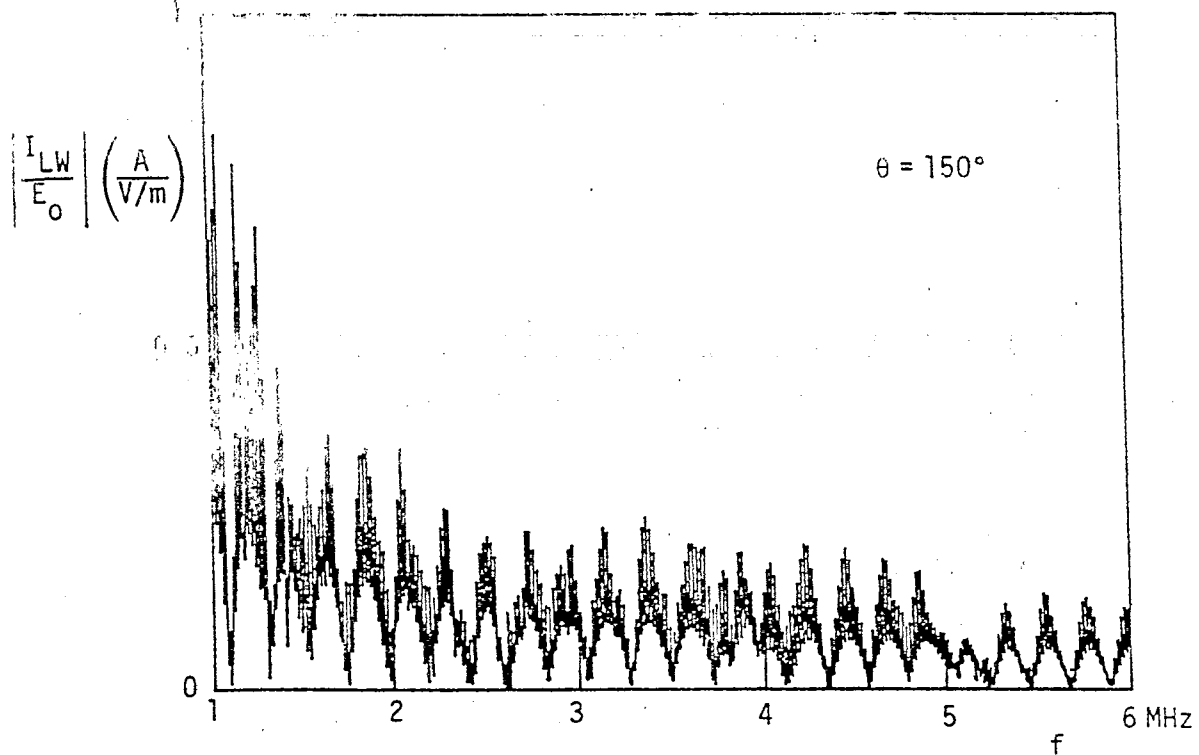
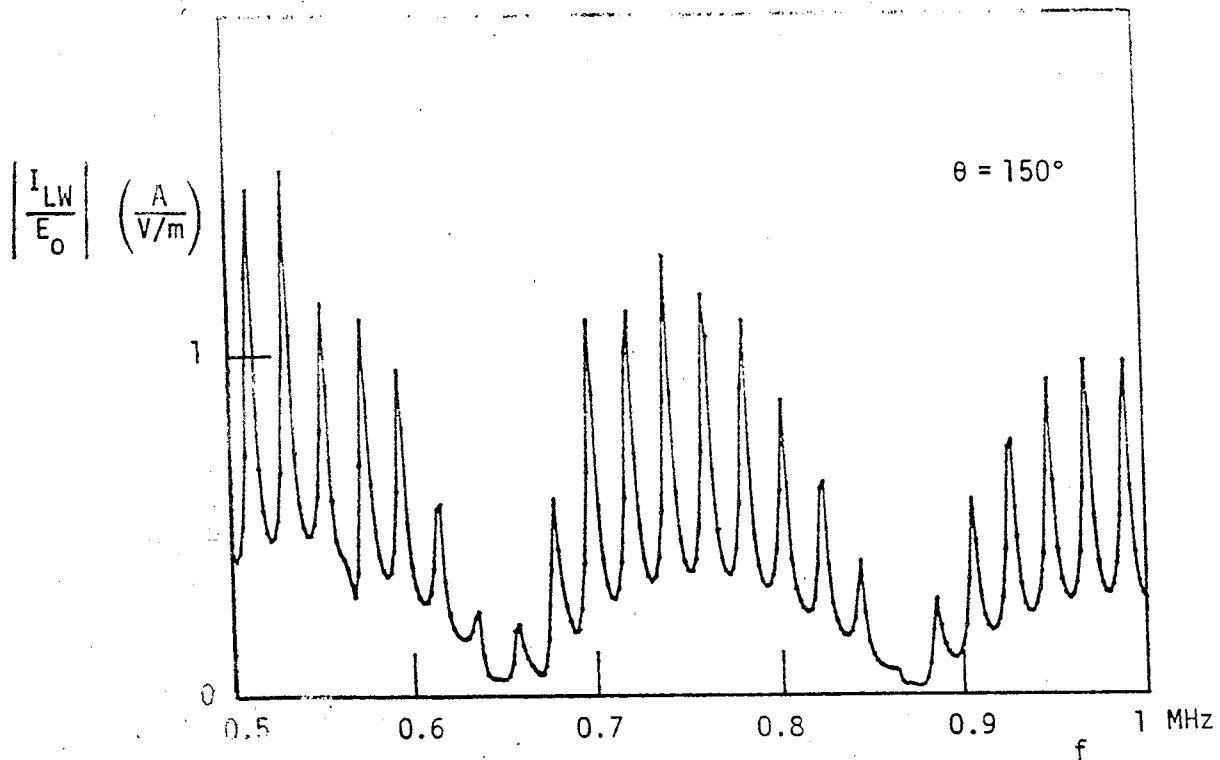
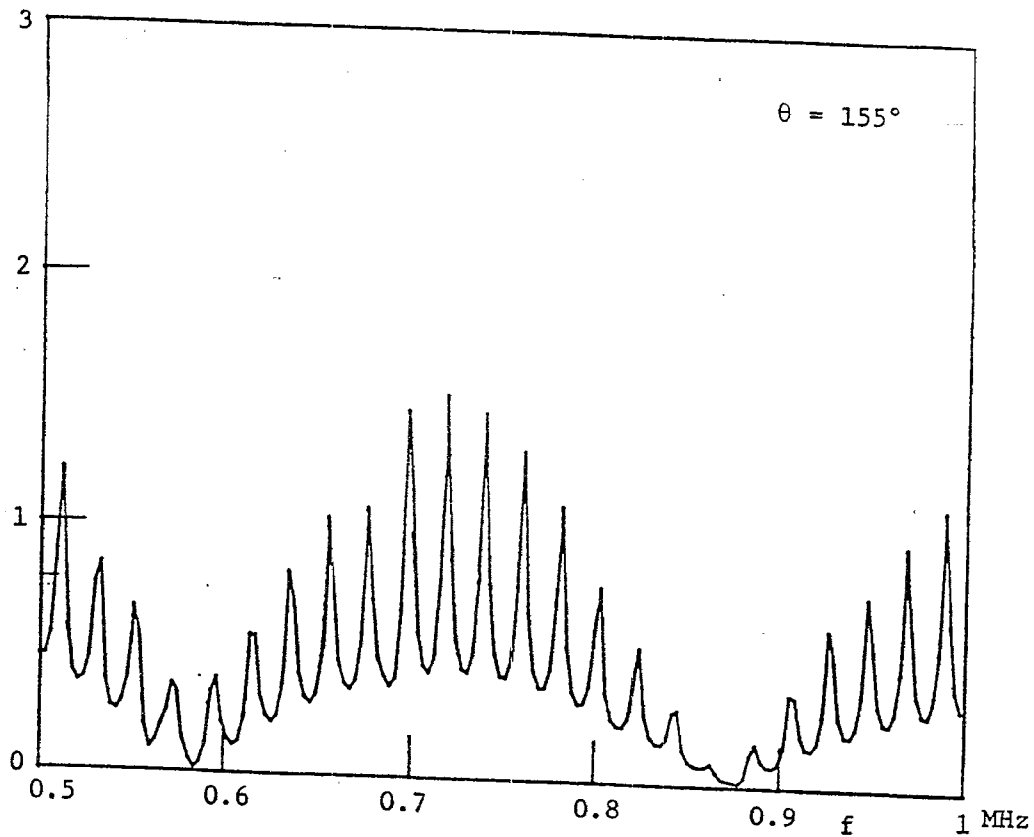


Figure 20. Magnitude of I_{LW} in the frequency ranges of 0.5-1 MHz and 1-6 MHz for $\theta=150^\circ$.

$$\left| \frac{I_{LW}}{E_o} \right| \left(\frac{A}{V/m} \right)$$



$$\left| \frac{I_{LW}}{E_o} \right| \left(\frac{A}{V/m} \right)$$

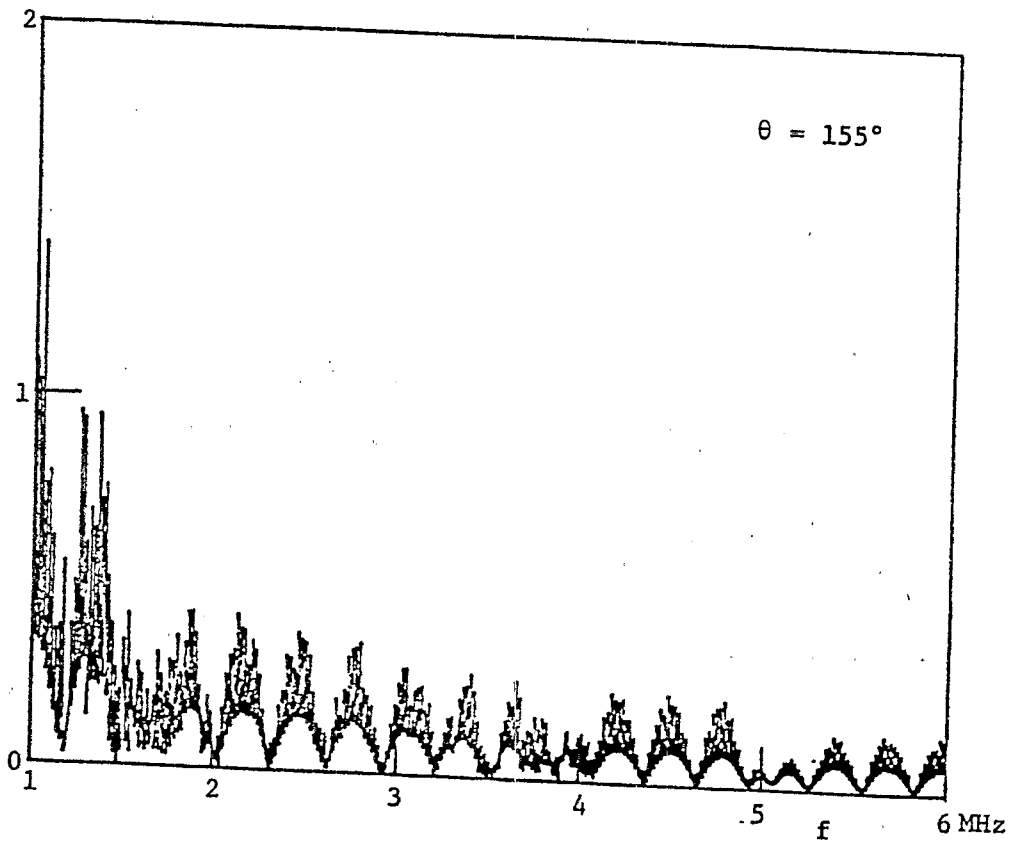
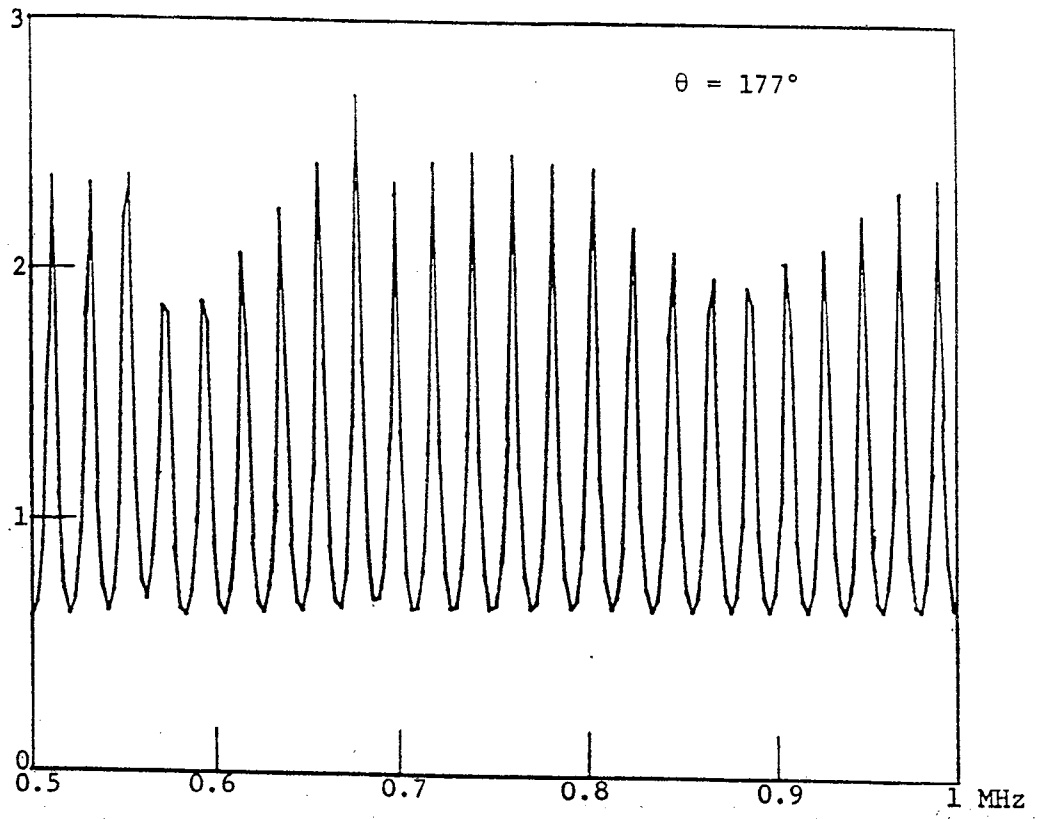


Figure 21. Magnitude of I_{LW} in the frequency ranges of 0.5-1 MHz and 1-6 MHz for $\theta=155^\circ$.

$$\left| \frac{I_{LW}}{E_0} \right| \left(\frac{A}{V/m} \right)$$



$$\left| \frac{I_{LW}}{E_0} \right| \left(\frac{A}{V/m} \right)$$

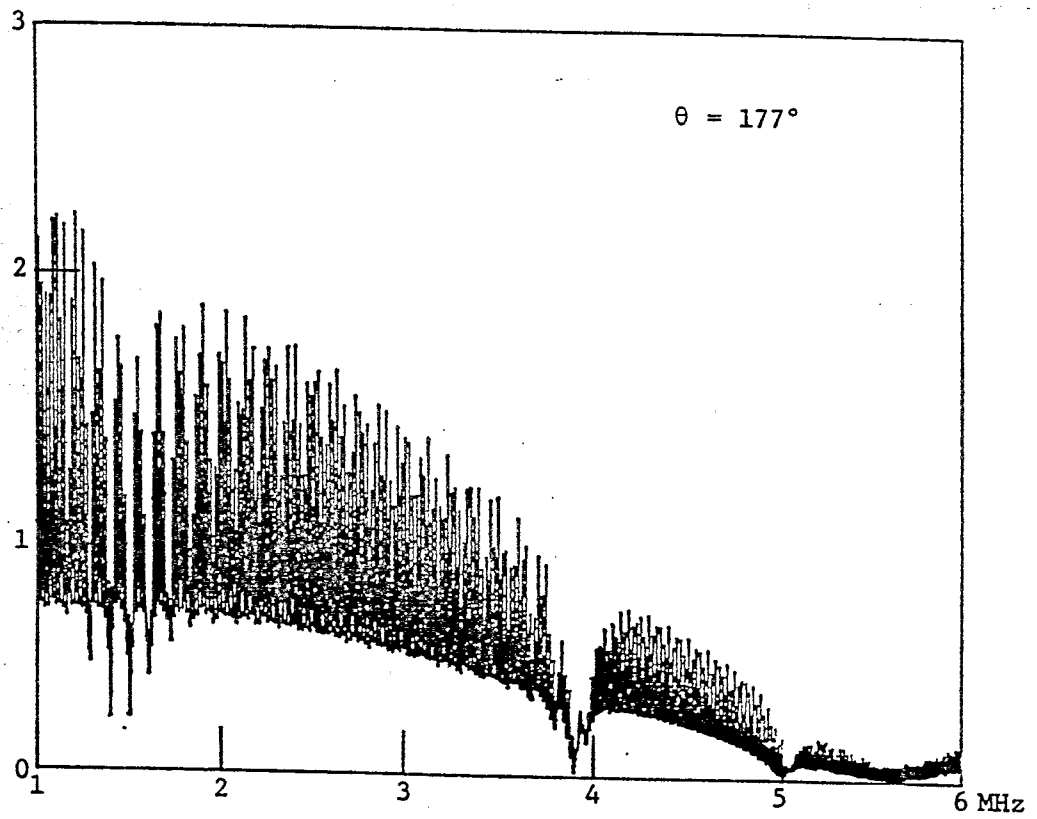


Figure 22. Magnitude of I_{LW} in the frequency ranges of 0.5-1 MHz and 1-6 MHz for $\theta = 177^\circ$.

SECTION IV

COMPARISON WITH EXISTING RESULTS

The purpose of this section is to compare numerical results obtained using the formulation of this report with those obtained in Reference 2. As mentioned previously, the difference in the two formulations is confined to the reflection coefficient $R(\theta, \xi)$. The results in Reference 2 are obtained from those presented here by putting $R(\theta, \xi) = 1$ and $P_1(\theta) = P_2(\theta) = 1$.

Figures 23 and 24 are typical examples of the differences when the incident field is not near grazing. As can be seen from these curves, the differences are small ($\leq 20\%$). For most practical purposes the results can be viewed as identical.

Figures 25 and 26 show some cases of what happens at near grazing angles of incidence. In this case the formulation of Reference 2 predicts a too large wire current response. For $\theta = 177^\circ$ this overestimation amounts to about a factor of two. For angles closer to $\theta = 180^\circ$ this factor is even larger.

Direct comparisons between numerical results obtained in Reference 5 and the results of this report are difficult since the aircraft are different (TACAMO versus E-4B) and since the antenna wires are deployed in different manners. We therefore limit the comparison to the qualitative comments made about the formulation.

The quantities presented in Reference 4 refer to the induced current and charge densities on the aircraft skin itself. These quantities have not been calculated here since our main interest lies in the antenna wire current itself. No direct comparison of numerical results is therefore made.

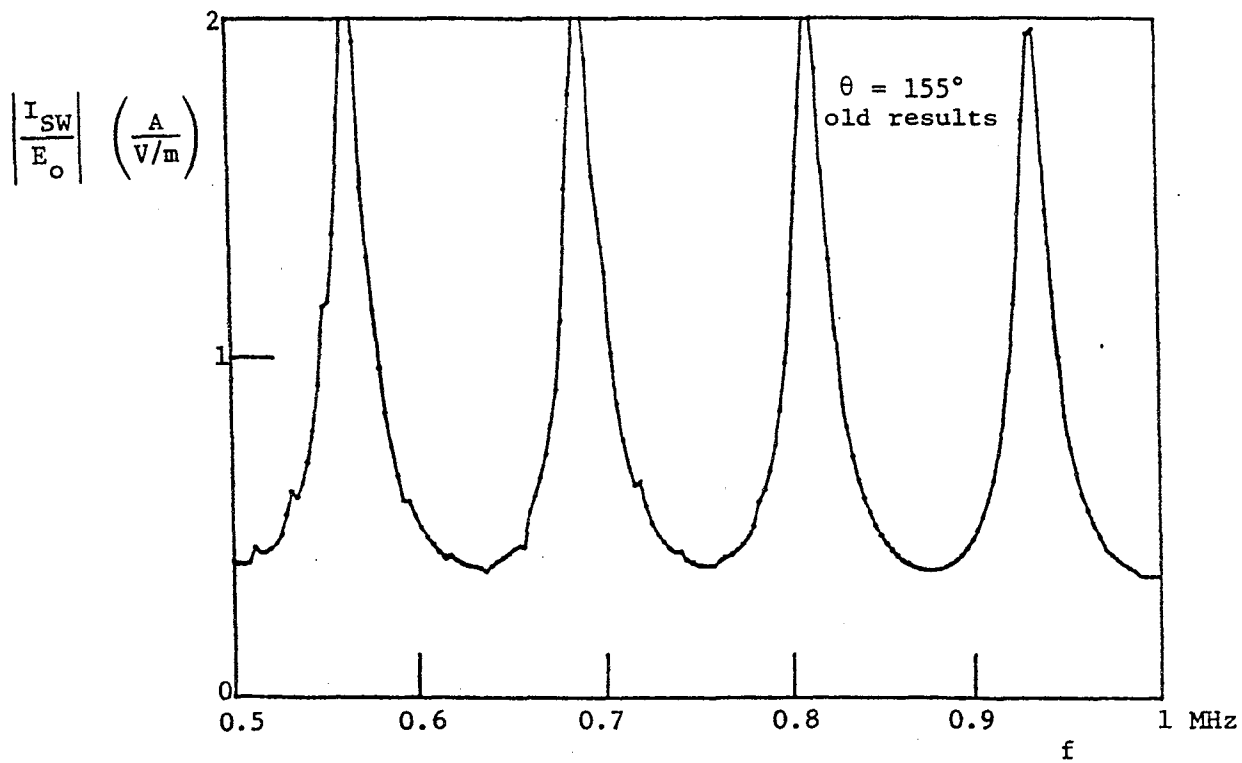
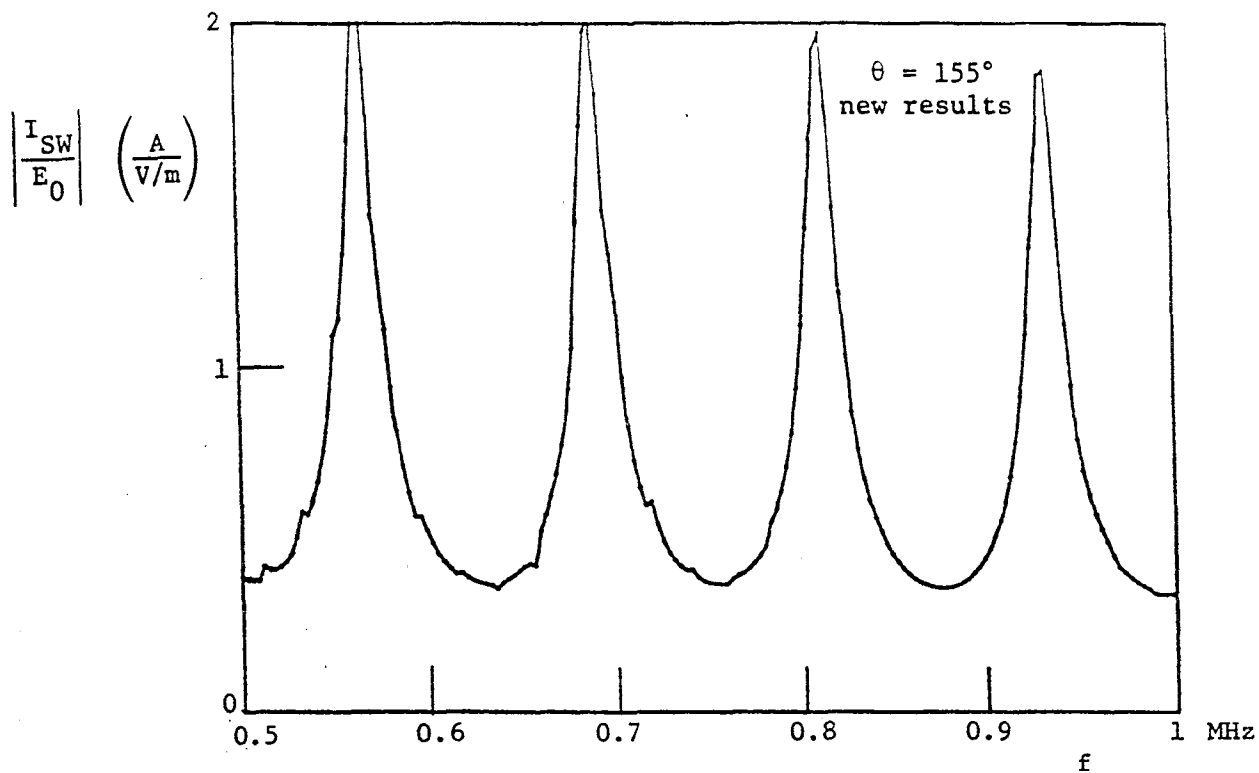


Figure 23. Comparison of the new results with the old results of $|I_{SW}|$ in the frequency range of 0.5 - 1 MHz for $\theta = 155^\circ$.

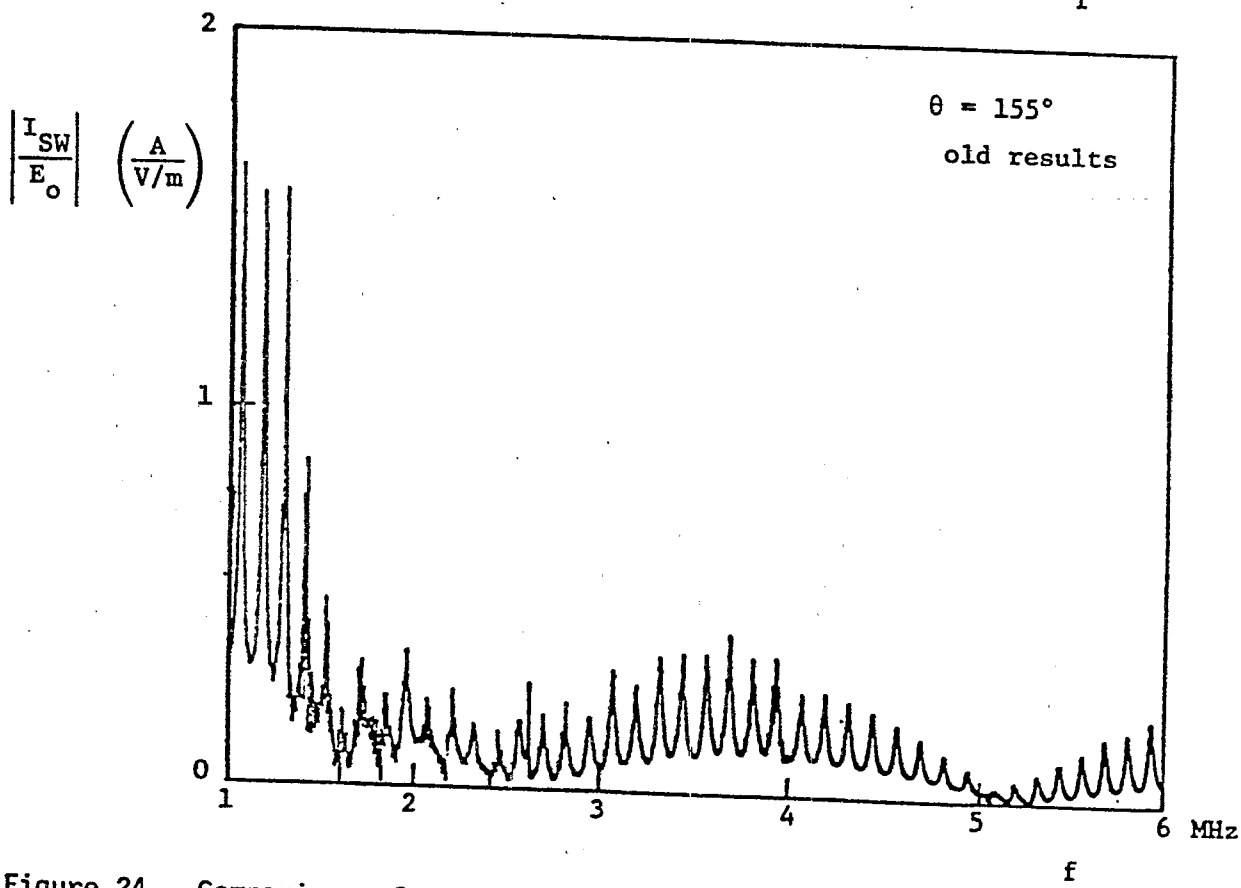
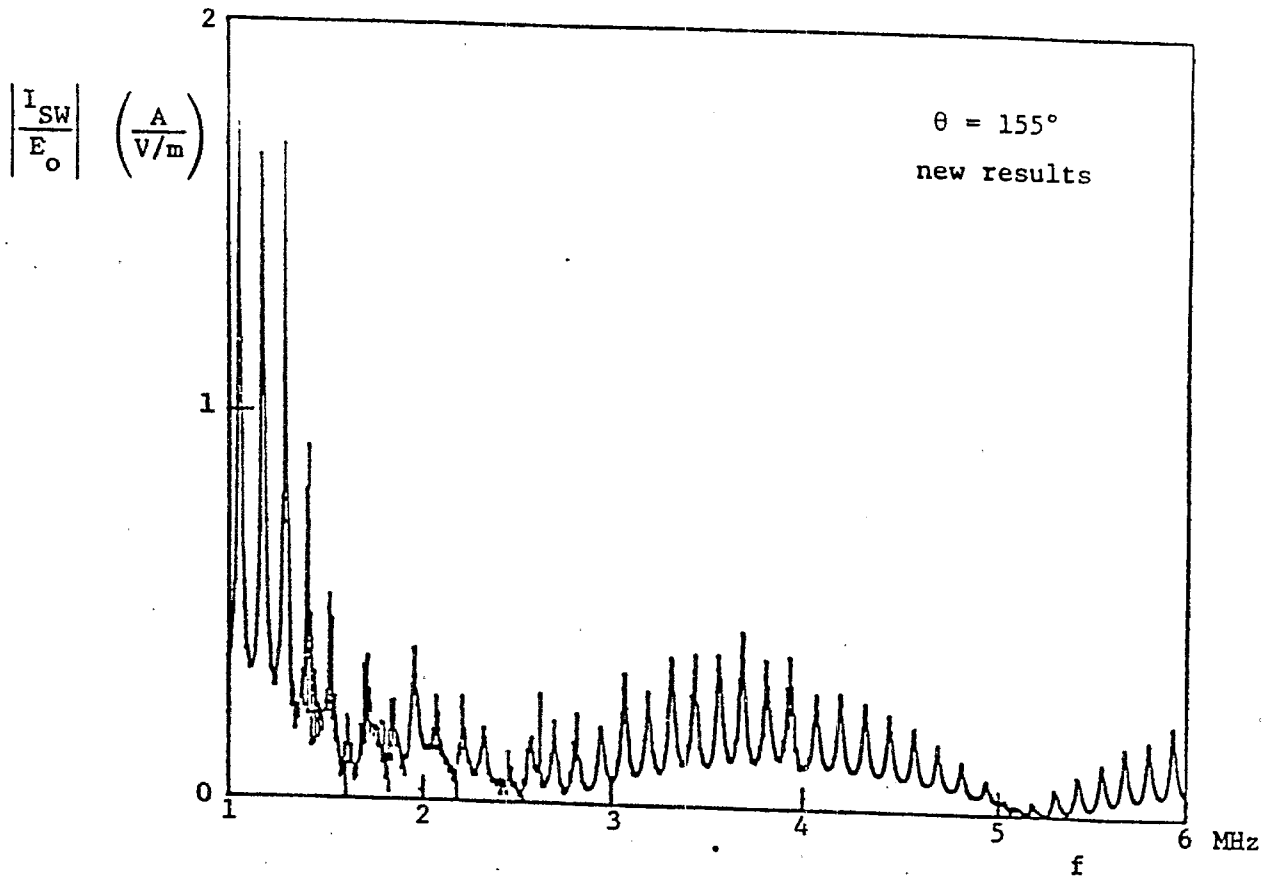


Figure 24. Comparison of the new results with the old results of $|I_{SW}|$ in the frequency range of 1 - 6 MHz for $\theta = 155^\circ$.

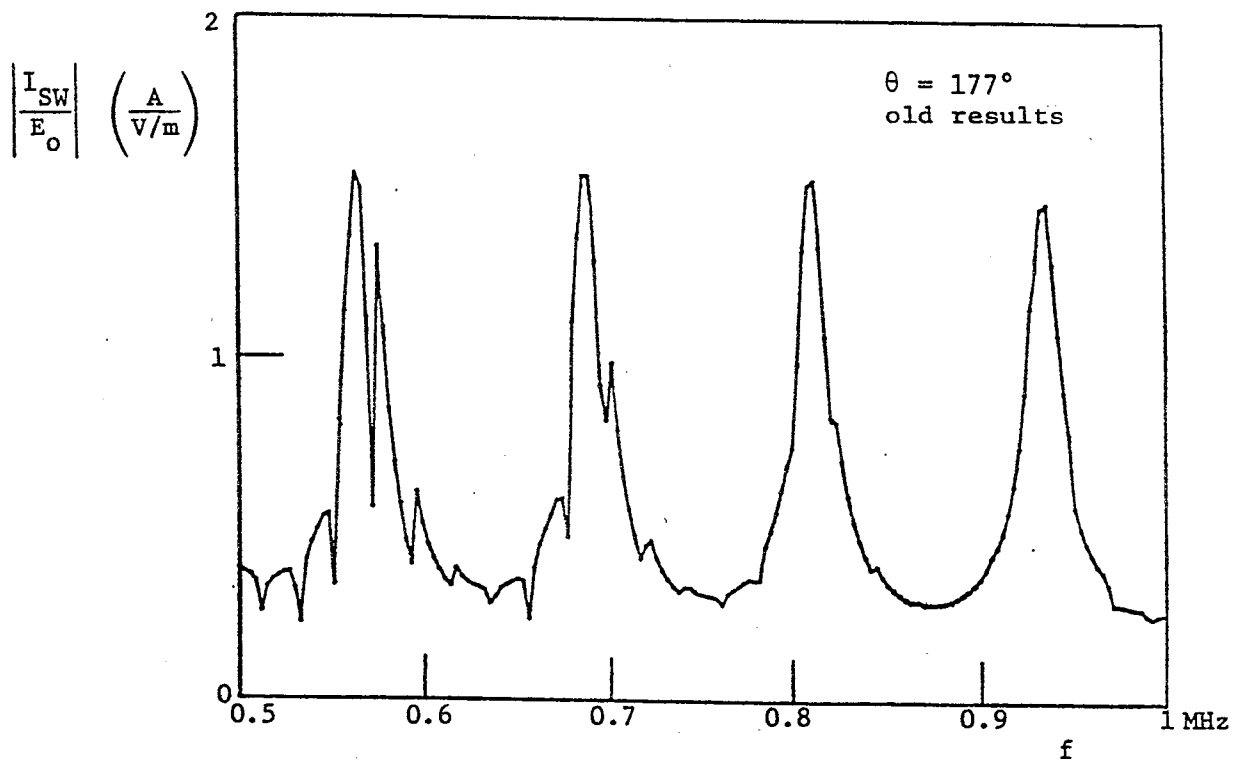
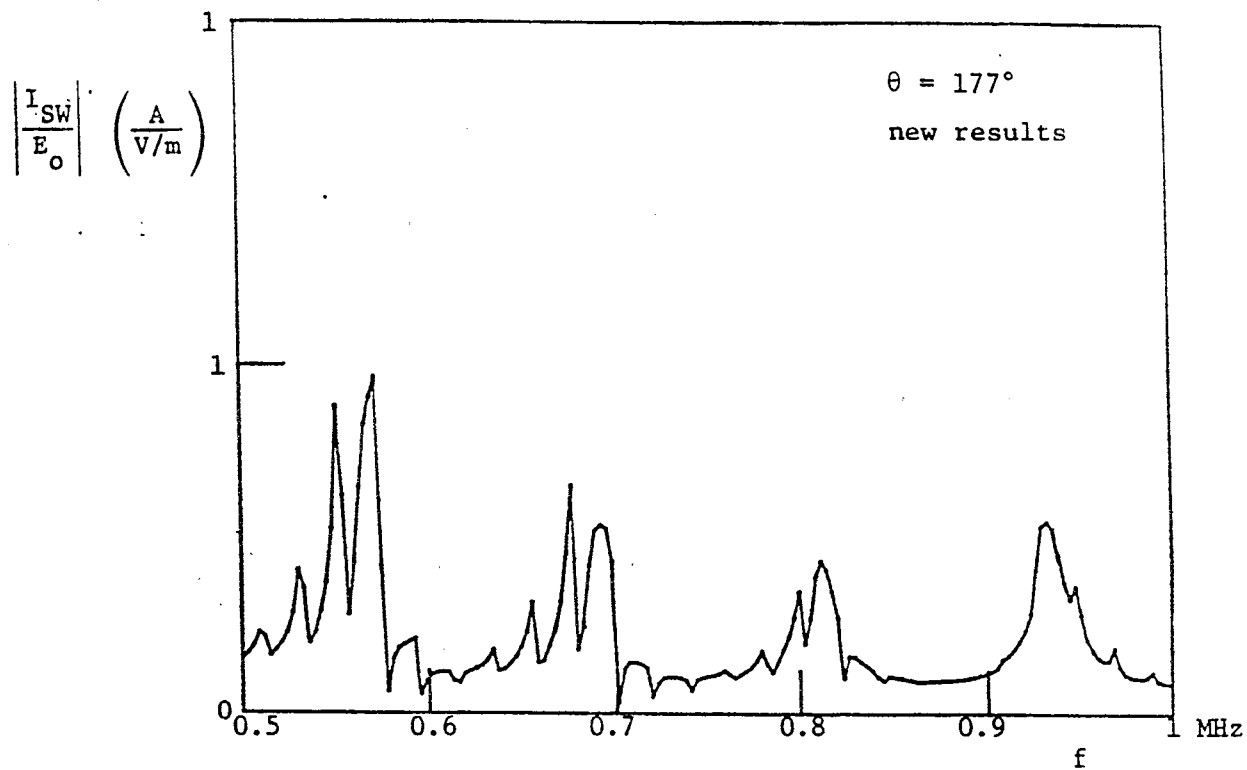


Figure 25. Comparison of the new results with the old results of $|I_{SW}|$ in the frequency range of 0.5-1 MHz for $\theta = 177^\circ$.

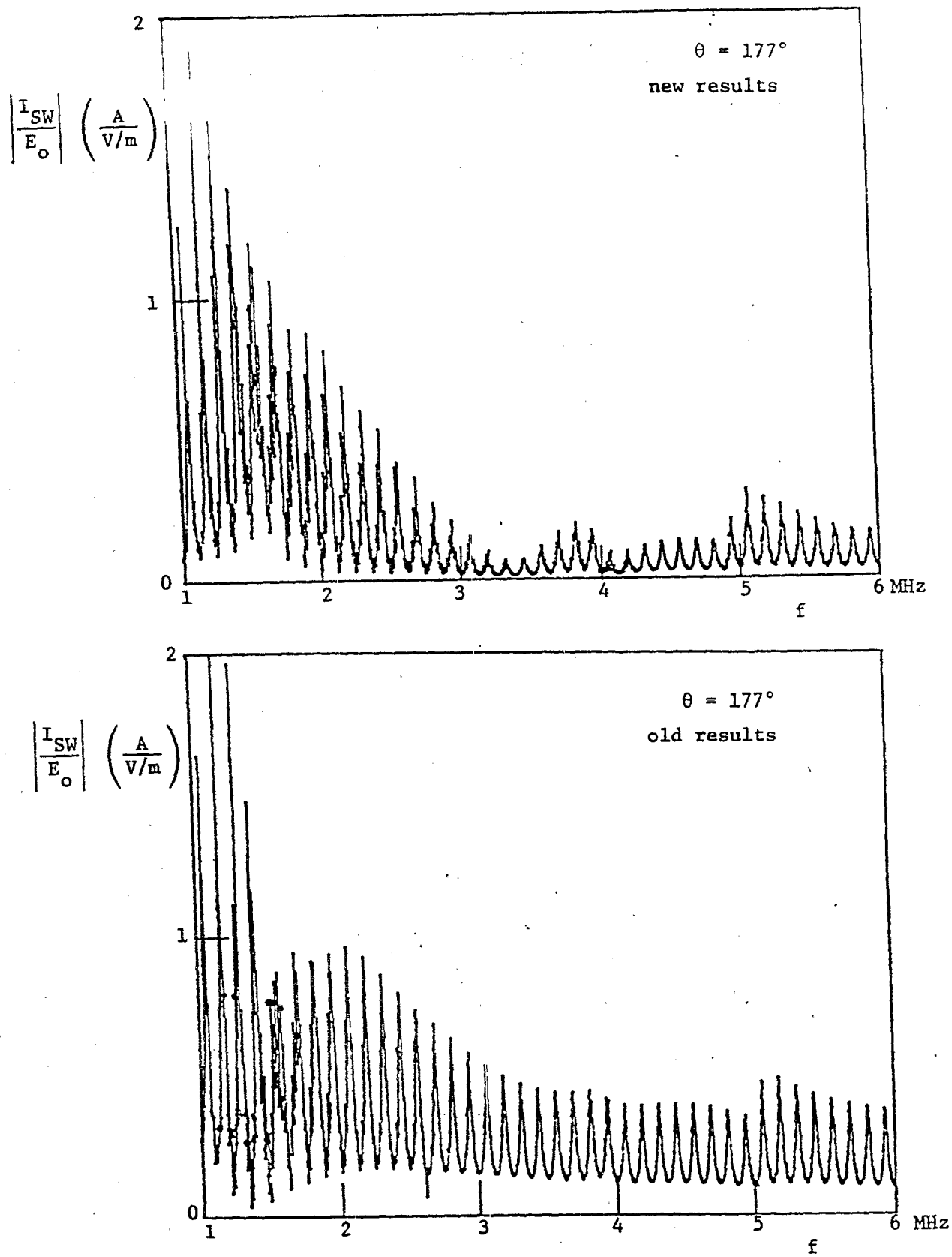


Figure 26. Comparison of the new results with the old results of $|I_{SW}|$ in the frequency range of 1-6 MHz for $\theta = 177^\circ$.

SECTION V

COMPARISON OF WIRE RESPONSES TO DIFFERENT EXCITATION MECHANISMS

The antenna wire currents can be thought of as a superposition of three different cases, namely

- aircraft only illuminated (wires present but not illuminated)
- short wire only illuminated (aircraft and long wire present but not illuminated)
- long wire only illuminated (aircraft and short wire present but not illuminated)

A schematic drawing of this decomposition is shown in Figure 27. The natural question that arises is "What is the relative importance of each one of these three excitation mechanisms?" The purposes for answering this question are

- aid in reaching conclusions about the fidelity of different simulation schemes
- aid in understanding how the wires are excited
- aid in calculating the transient response of the wires

To simplify the analysis and the interpretation of the results we will let L_1 and L_2 tend to infinity. This way all the resonances due to multiple reflections at the two ends of the wires will not be present in the results. Three different angles of incidence are presented in this report, namely $\theta = 30^\circ$, 155° , and 177° . The results of the comparison are presented in Figures 28 through 39.

In Figures 28,32, and 36 we compare the response of the short wire when both wires and the aircraft are excited with the response of the same wire when only the short wire and the aircraft are excited. The differences between the responses in these curves are small pointing to the fact that the long wire has a small influence upon the response of the short wire. Similarly, Figures 30,34 and 38 show that the short wire has a small influence upon the response of the long wire. Thus, when simulating or analyzing the response of the short (long) wire one can neglect the presence of the long (short) wire.

The next issue to deal with is the relative contribution of wire and aircraft illumination to the excitation of a given wire. In Figures 29,33, and 37 we compare the response of the short wire when only the aircraft is excited to the response of the same wire when only the short wire is excited. For ease of computations the response of both wires being excited is shown in the figures. The results from Figures 28,32, and 36 however imply that the long wire has a negligible influence on the short wire response. Similarly, Figures 31,35, and 39 show the response of the long wire when only the aircraft is excited and when the wire is excited. The results presented in Figures 29, 31, 33, 35, 37 and 39 show that the excitation of the respective wire is the dominating factor in the wire response for low frequencies (below 1 MHz). The effect of the aircraft excitation appears primarily in the aircraft resonance region. The results also show that the wire excitation is the dominant excitation mechanism even for high frequencies when the incident wave hits the wires and aircraft "from behind" i.e., is around 180° .

Many of these results can be understood by considering impedance conditions. The antenna wires respond approximately as continuously excited transmission lines with a large characteristic impedance. Each portion (or stick member) of the aircraft on the other hand acts approximately as a transmission line with a much lower characteristic impedance. Thus, there is a large impedance mismatch between the transmission lines representing the wires and the aircraft. This gives rise to reflections at the intersection between the different lines. In particular, any current on the aircraft sees a large impedance at each wire thus preventing it to get onto the wire. Only resonance phenomena on the aircraft can change this situation. On the other hand, the aircraft presents a low impedance to the wire currents. Thus, there is a voltage minimum (current maximum) on each wire at its attachment point to the aircraft.

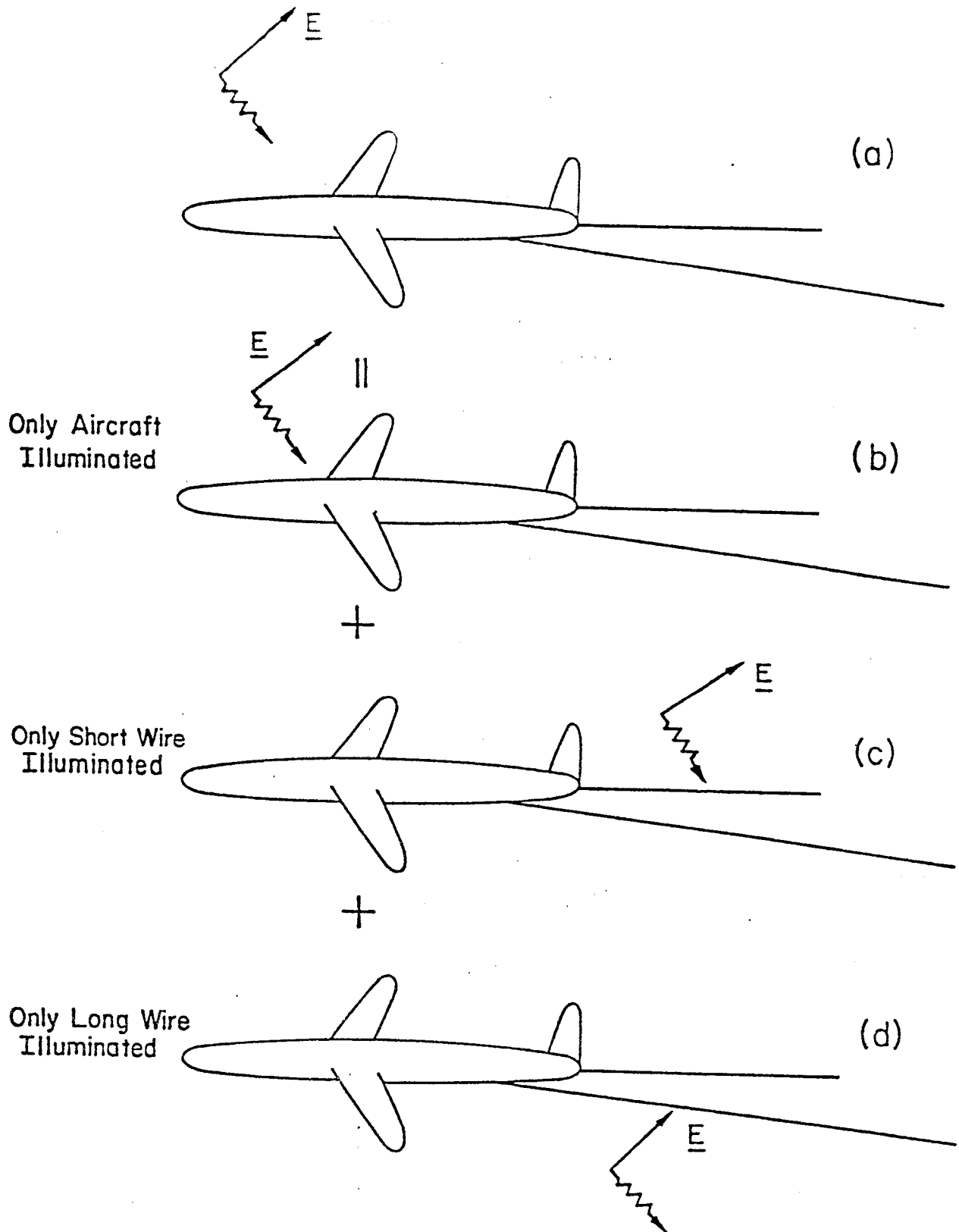


Figure 27. Decomposition of the actual excitation problem into excitation of the aircraft itself, the short antenna wire, and the long antenna wire.

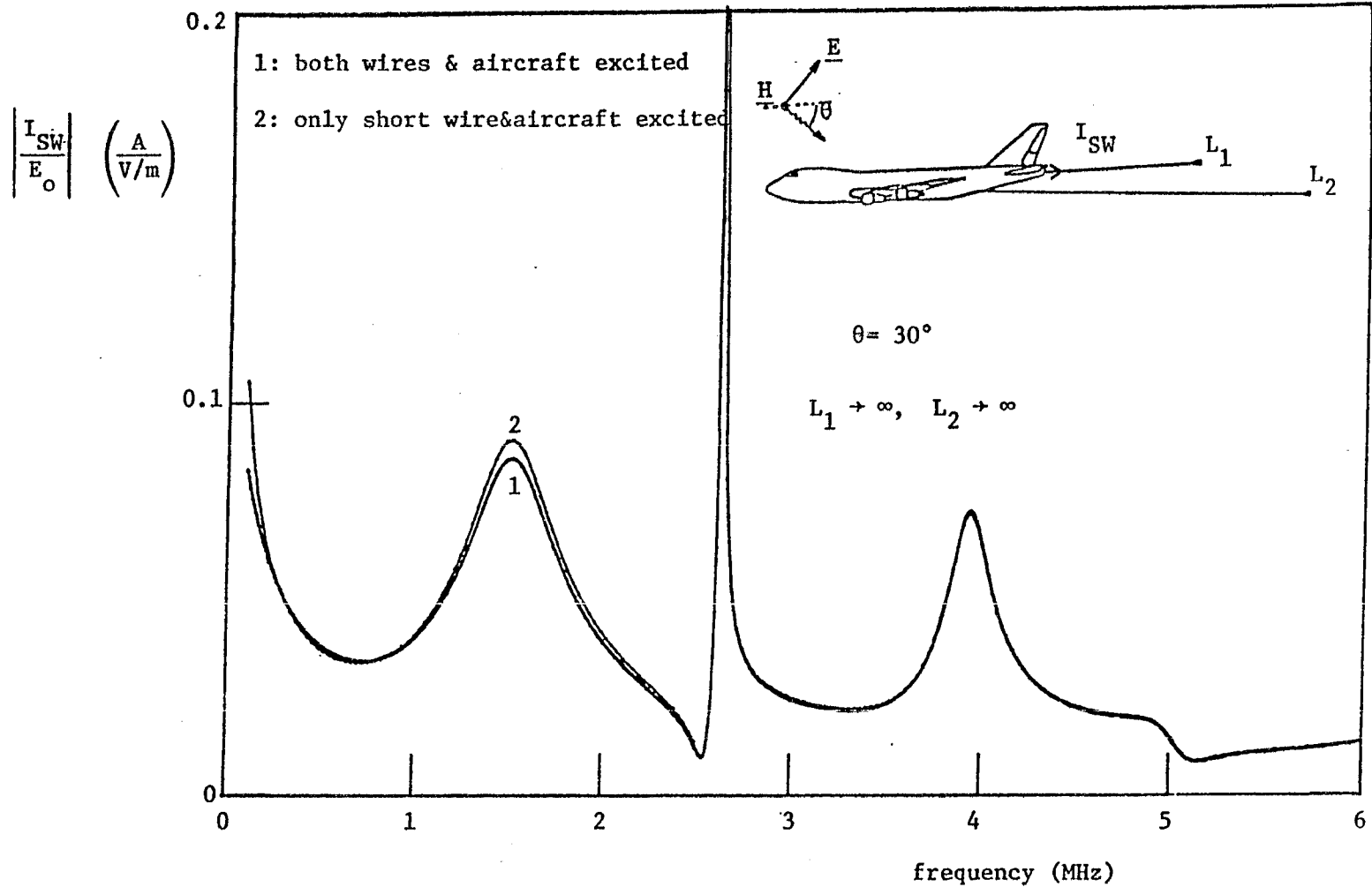


Figure 28. Comparison of $|I_{SW}|$ when both wires and the aircraft are excited with that when only the short wire and the aircraft are excited for $\theta = 30^\circ$ and $L_1 = L_2 \rightarrow \infty$.

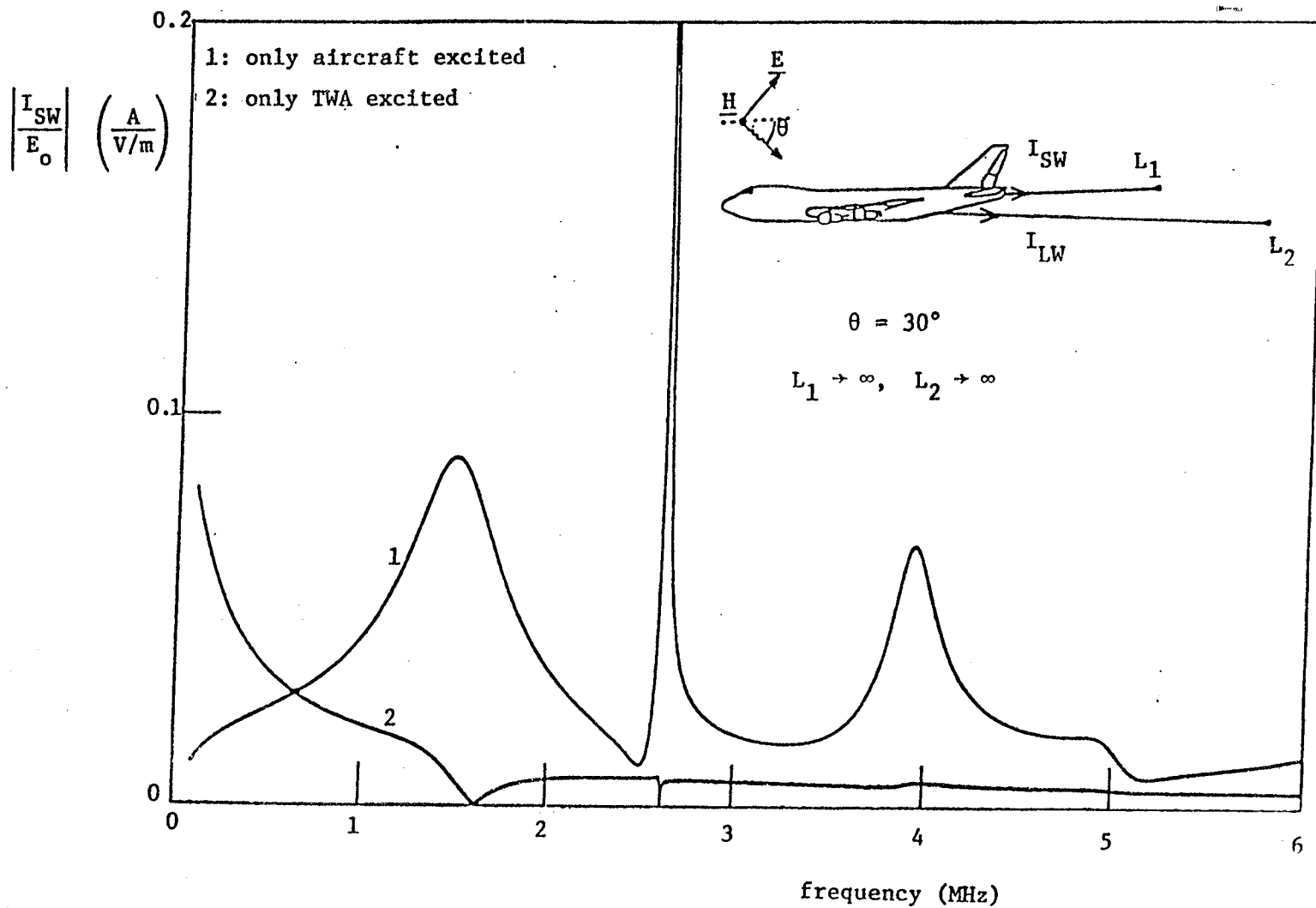


Figure 29. Comparison of $|I_{SW}|$ when only the aircraft is excited with that when only the wires are excited for $\theta = 30^\circ$ and $L_1 = L_2 \rightarrow \infty$.

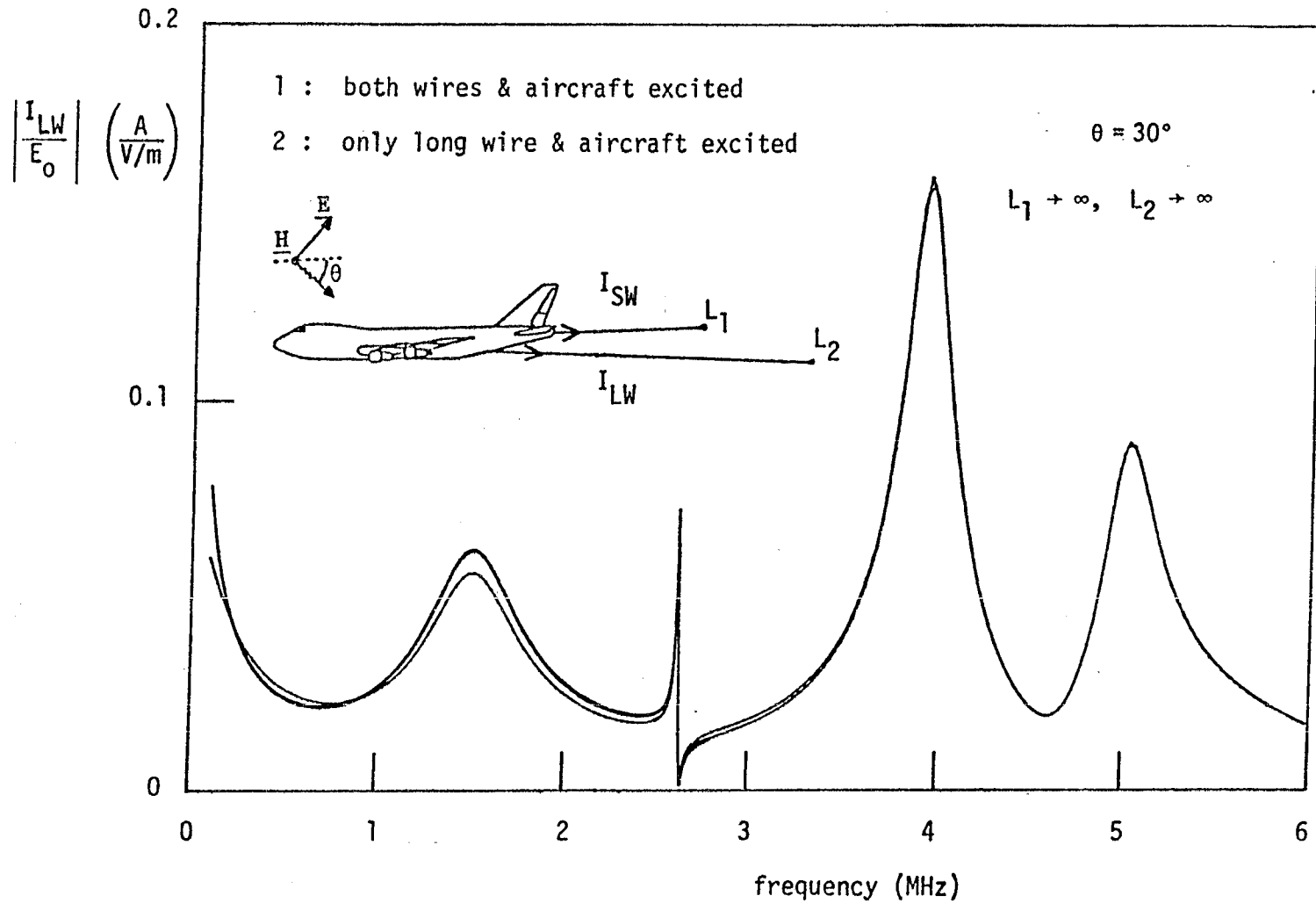


Figure 30. Comparison of $|I_{LW}|$ when both wires and the aircraft are excited with that when only the long wire and the aircraft are excited for $\theta = 30^\circ$ and $L_1 = L_2 \rightarrow \infty$.

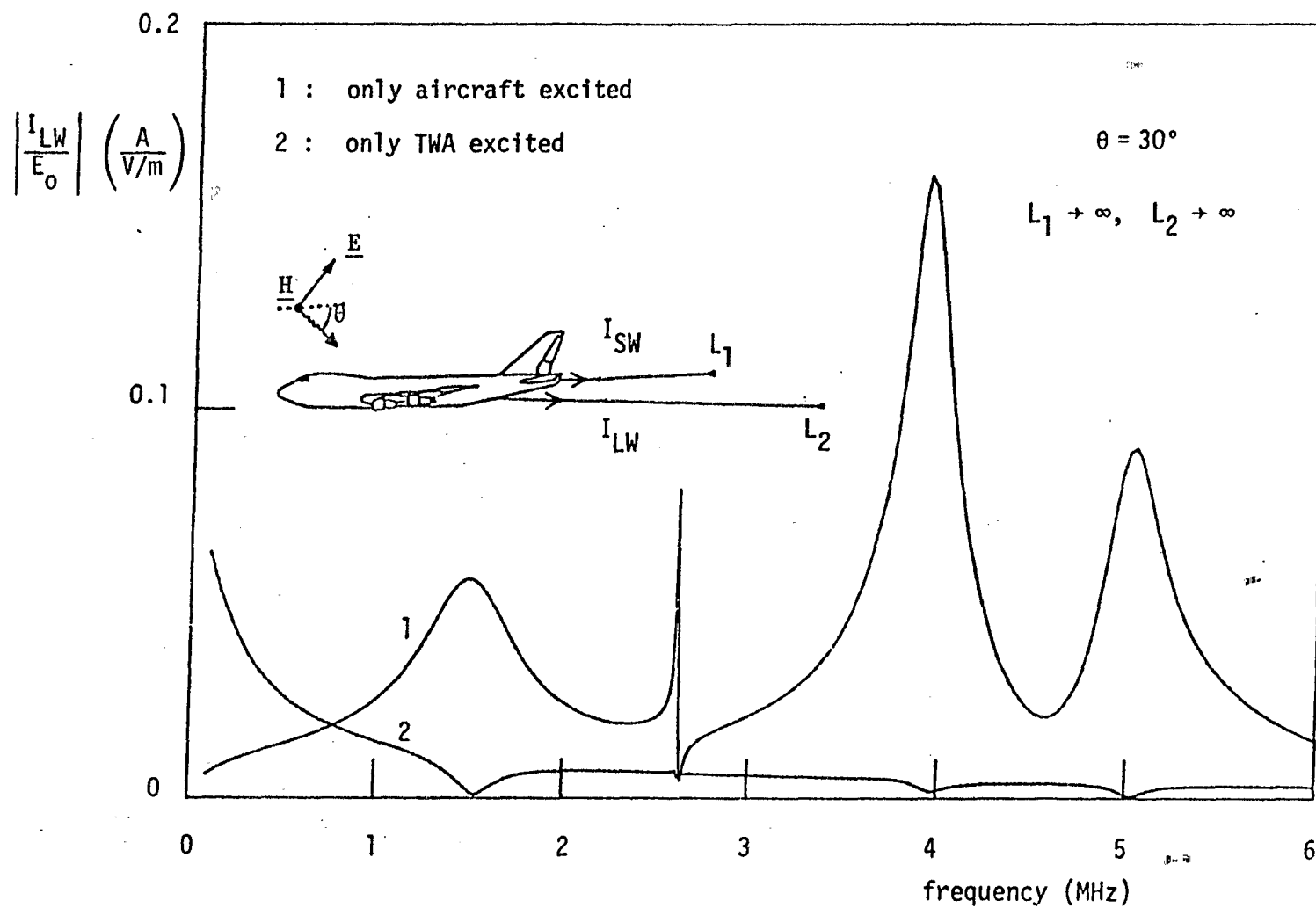


Figure 31. Comparison of $|I_{LW}|$ when only the aircraft is excited with that when only the wires are excited for $\theta = 30^\circ$ and $L_1 = L_2 \rightarrow \infty$.

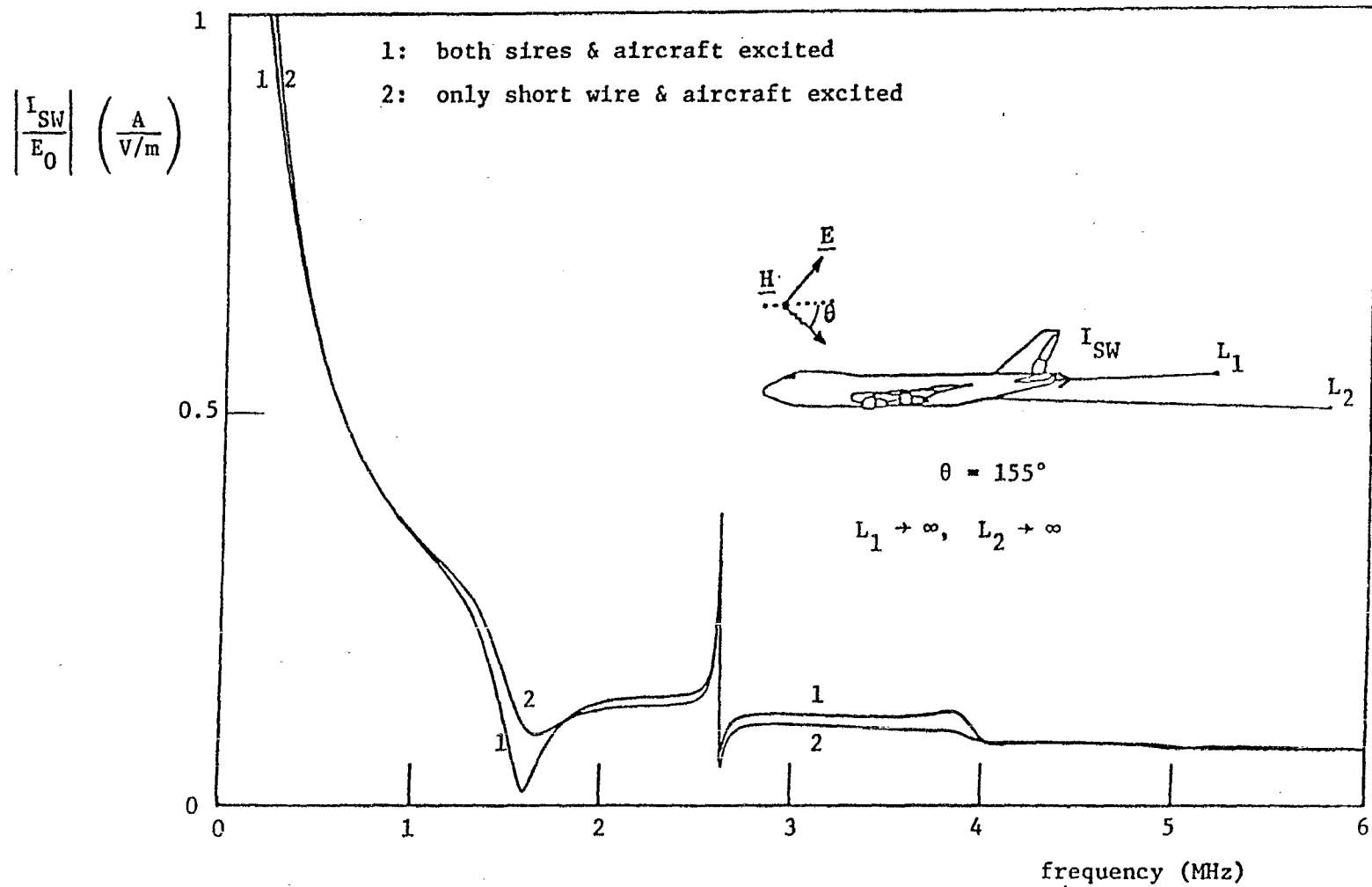


Figure 32. Comparison of $|I_{SW}|$ when both wires and the aircraft are excited with that when only the short wire and the aircraft are excited for $\theta=155^\circ$ and $L_1=L_2 \rightarrow \infty$.

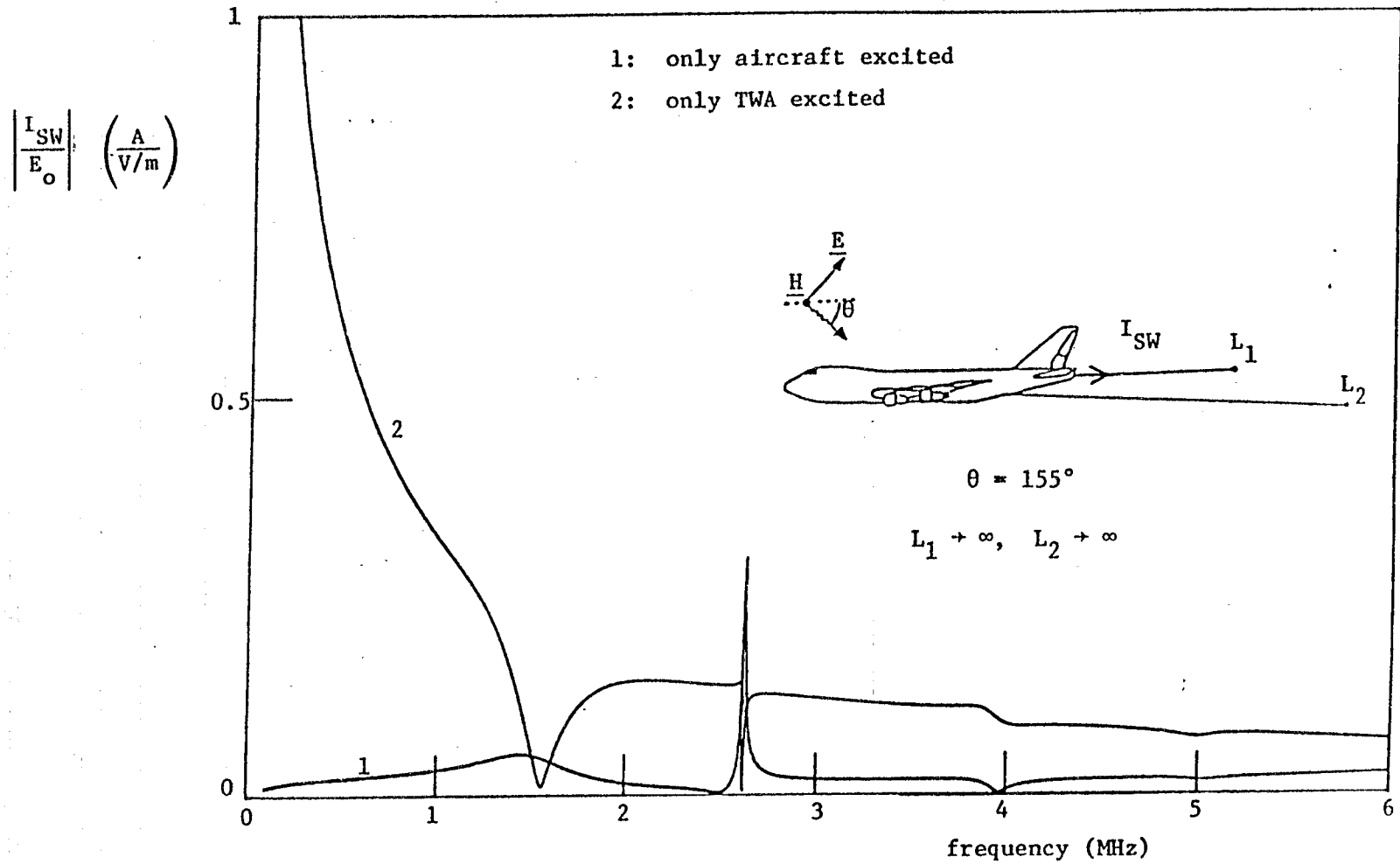


Figure 33. Comparison of $|I_{SW}|$ when only the aircraft is excited with that when only the wires are excited for $\theta=155^\circ$ and $L_1=L_2 \rightarrow \infty$.

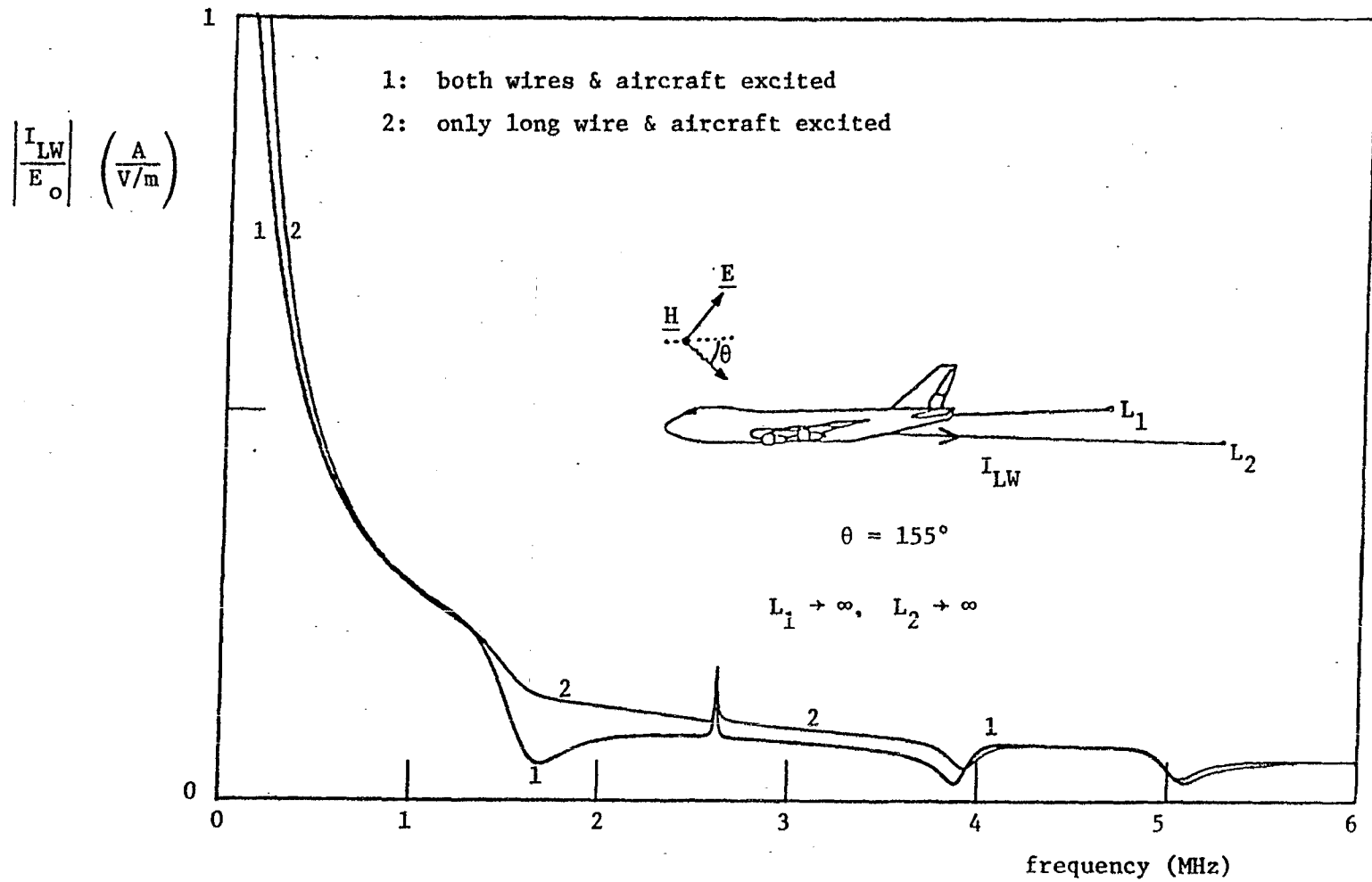


Figure 34. Comparison of $|I_{LW}|$ when both wires and the aircraft are excited with that when only the long wire and the aircraft are excited for $\theta=155^\circ$ and $L_1=L_2 \rightarrow \infty$.

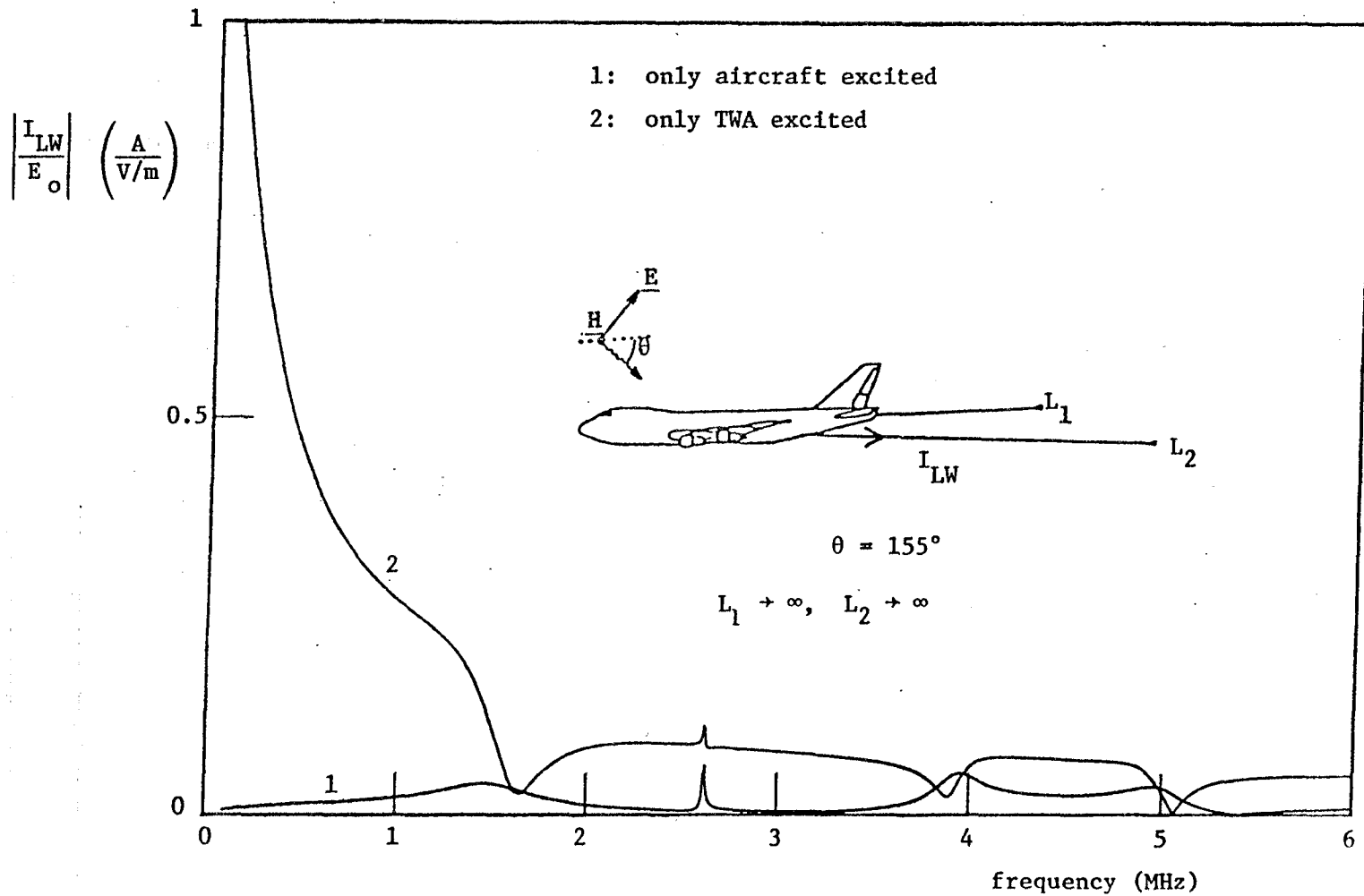


Figure 35. Comparison of $|I_{LW}|$ when only the aircraft is excited with that when only the wires are excited for $\theta=155^\circ$ and $L_1=L_2 \rightarrow \infty$.

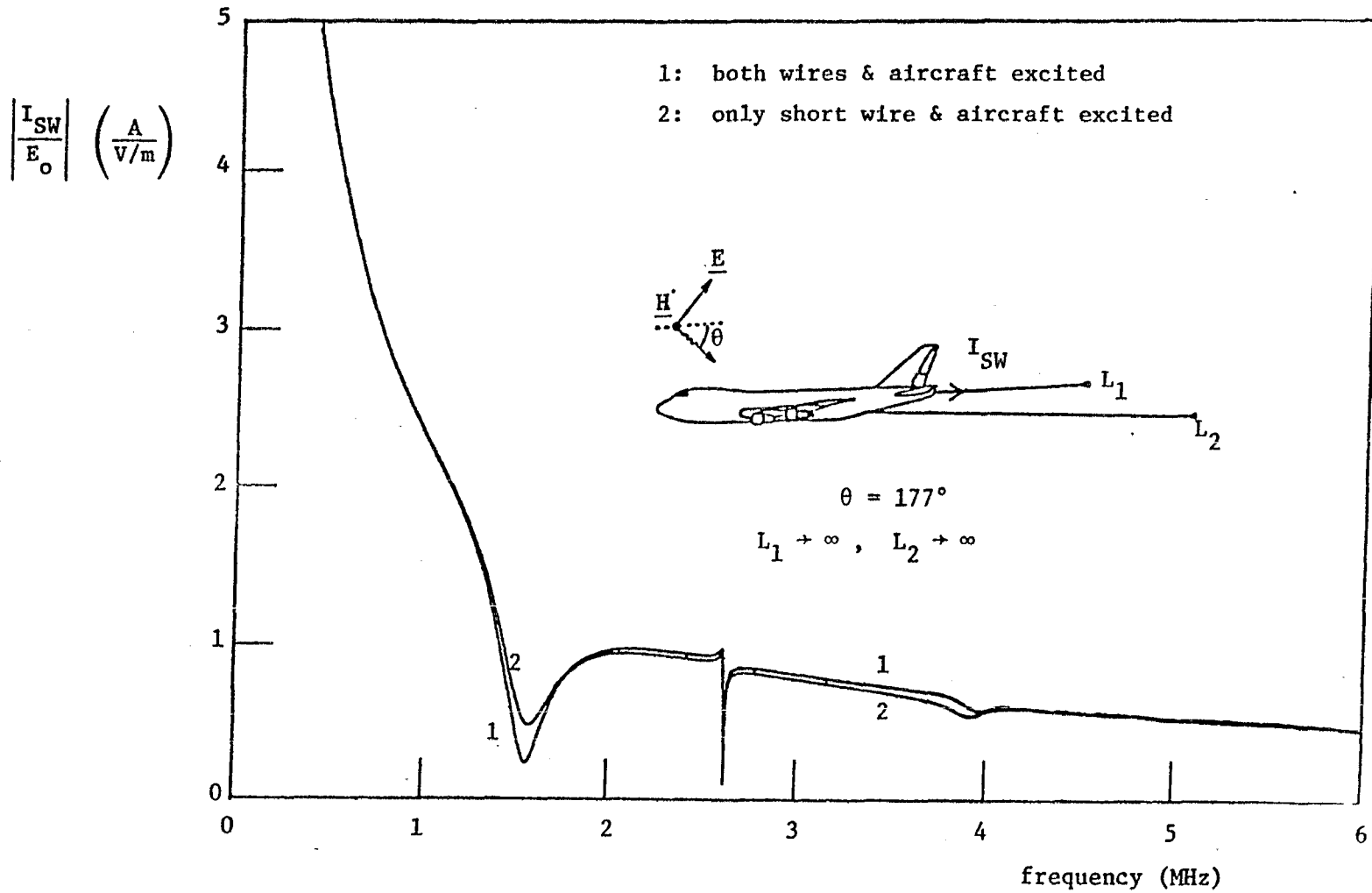


Figure 36. Comparison of $|I_{SW}|$ when both wires and the aircraft are excited with that when only the short wire and the aircraft are excited for $\theta=177^\circ$ and $L_1=L_2 \rightarrow \infty$.

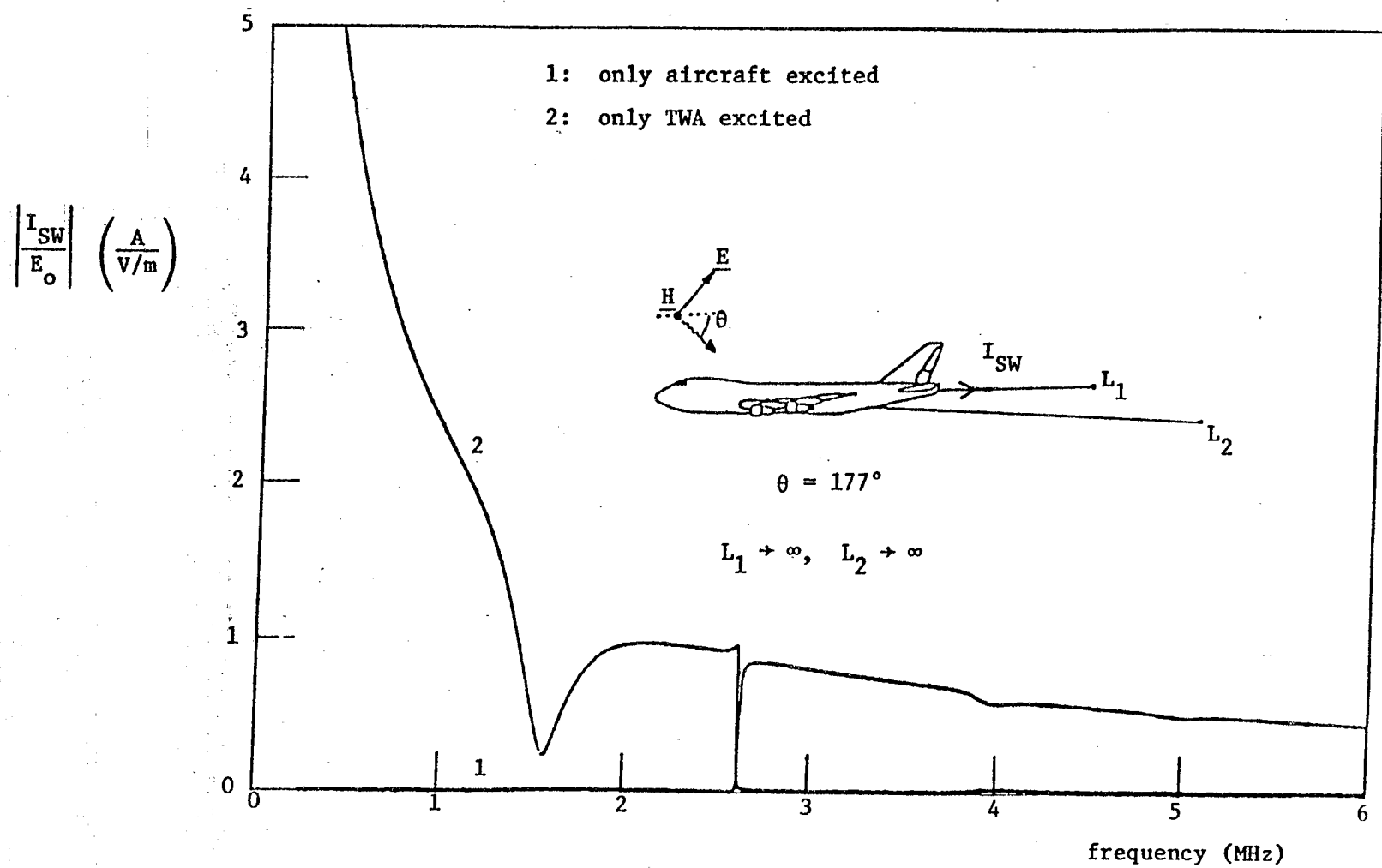


Figure 37. Comparison of $|I_{SW}|$ when only the aircraft is excited with that when only the wires are excited for $\theta=177^\circ$ and $L_1=L_2 \rightarrow \infty$.

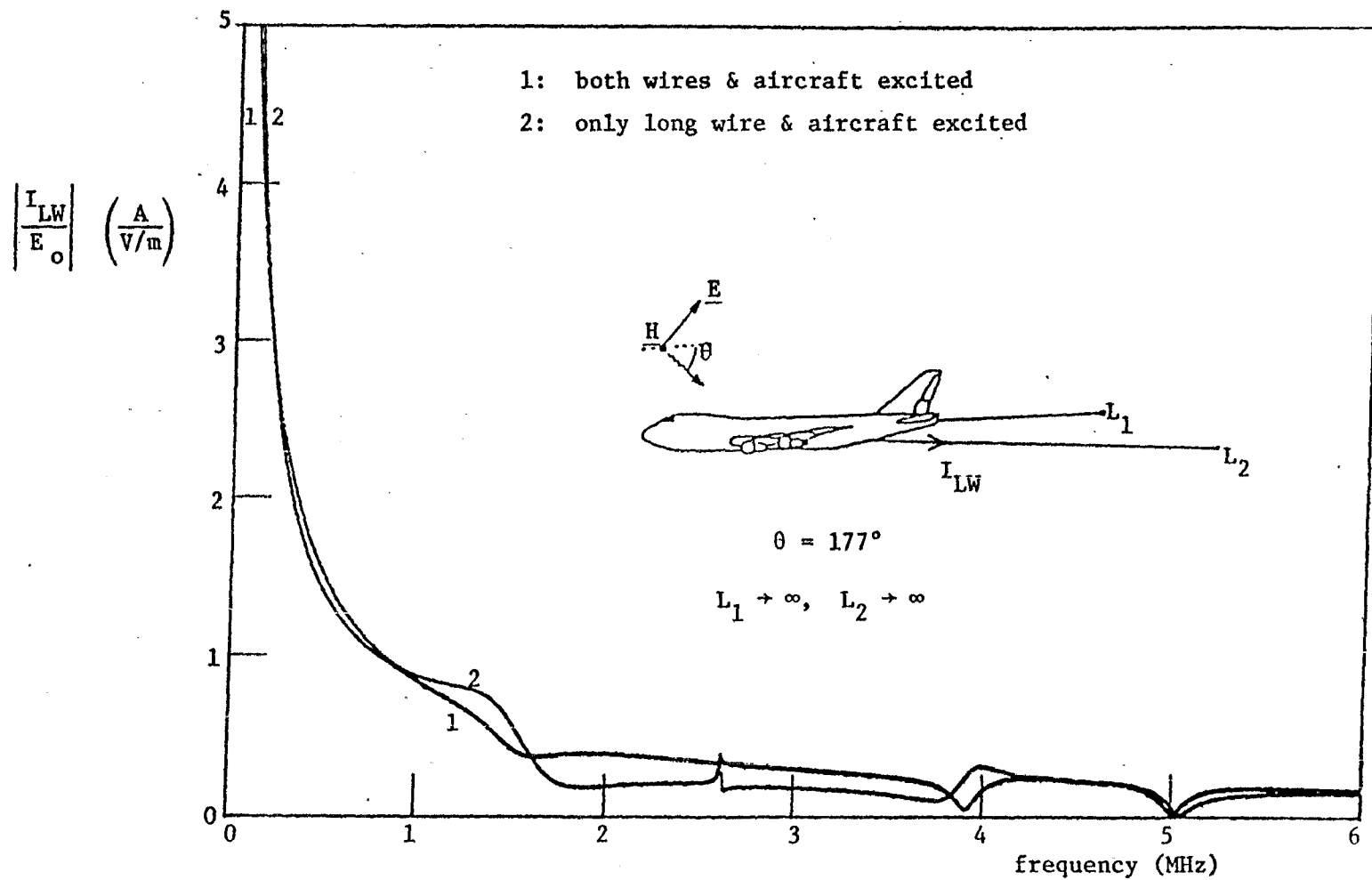


Figure 38. Comparison of $|I_{LW}|$ when both wires and the aircraft are excited with that when only the long wire and the aircraft are excited for $\theta=177^\circ$ and $L_1=L_2 \rightarrow \infty$.

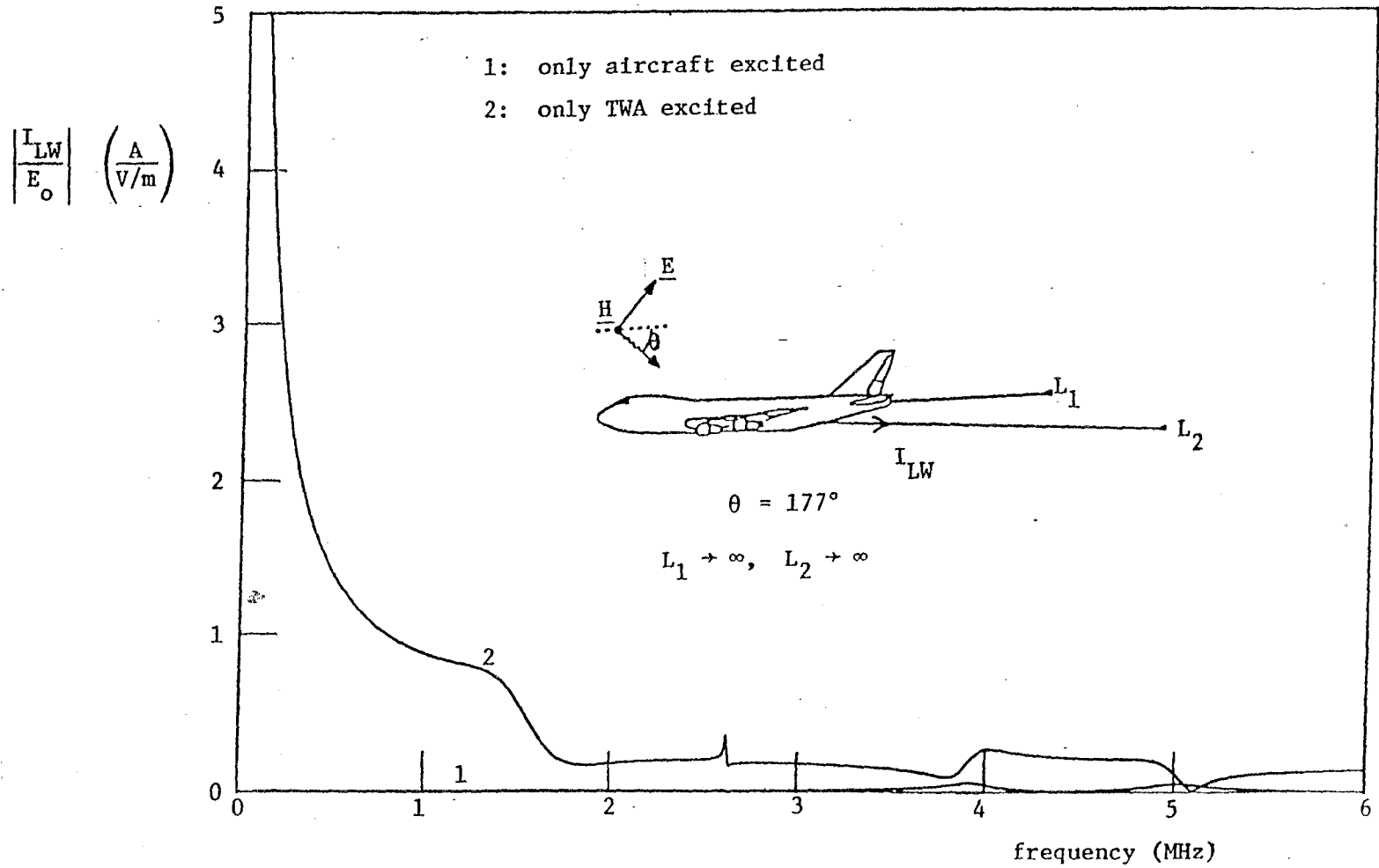


Figure 39. Comparison of $|I_{LW}|$ when only the aircraft is excited with that when only the wires are excited for $\theta=177^\circ$ and $L_1=L_2 \rightarrow \infty$.

SECTION VI
CONCLUSIONS

The frequency-domain response of the trailing-wire antenna has been calculated in this report. The results of the analysis can be summarized in the following manner

- The mutual coupling between the wires is weak. This conclusion is drawn from two observations regarding the results. First, the resonances observed for the short wire are dominated by the length of the short wire only whereas the resonances for the long wire are dominated by the length of the long wire. Second, the short wire response is due to the excitation of the aircraft and the short wire and the long wire response is due to the excitation of the aircraft and the long wire.
- The low frequency response of each wire is due to the excitation of the respective wire only. The excitation of the aircraft only influences the wire response in the aircraft resonance region.
- Angles of incidence near the grazing angle result in the largest response. Compared to other angles of incidence, values twice as large were found for these critical angles. It was also found that the response is dominated by the wire excitation for near grazing angles of incidence. The aircraft excitation has a minor influence in this case.
- Comparisons with results obtained in Reference 2 using a simplified theory show agreement within 20% for angles off near grazing. For near grazing angles, the simplified theory overestimates the response.

APPENDIX A

ANALYTICAL EXPRESSIONS FOR THE WIRE CURRENTS

The expressions derived in Section II for the wire currents are

$$I_{\text{ind}}^{\text{SW}} = I_S(0, \theta) - I_S(L_1, \theta)R(\pi - \theta, L_1)F_1 + K(1 - R_1F_1^2) \quad (\text{A1})$$

$$I_{\text{ind}}^{\text{LW}} = I_S(0, \phi) - I_S(L_2, \phi)R(\pi - \phi, L_2)F_2 \exp(jk\ell_4 \cos \theta) + M(1 - R_2F_2^2)$$

The quantities K, M, F_1, F_2, R_1 , and R_2 take the following form

$$K = \frac{Q_0 \Omega / [j\psi(1 + F_1'^2)]}{\tan(k\ell_1) + 2 \tan(k\ell_2) + \tan[k(\ell_3 + \ell_4 + \ell_5)] + \frac{\Omega}{j\psi} \left(\frac{1 - R_2F_2^2}{1 + F_2'^2} T_3 + \frac{1 - R_1F_1^2}{1 + F_1'^2} T_4 \right)} \quad (\text{A2})$$

$$M = \frac{(1 + F_1'^2)K + A_0 \Omega / (j\psi)}{(1 + F_2'^2) T_2 \cos(k\ell_4)}$$

$$\frac{\cos \theta I_0(\ell_4, \theta) \Omega / \psi + [\cos \phi I_S(0, \phi) + I_S(L_2, \phi)F_2P_2(\pi - \phi)] \exp(jk\ell_4 \cos \theta)}{1 + F_2'^2} \quad (\text{A3})$$

$$Q_0 = \frac{[\tan(k\ell_1) + 2 \tan(k\ell_2)] \tan(k\ell_3) - 1}{[1 - \tan(k\ell_4) \tan(k\ell_5)] [1 - \tan(k\ell_3) \tan(k\ell_4 + k\ell_5)]} P_0 \quad (\text{A4})$$

$$P_0 = W_0 - \frac{j\psi}{\Omega} [T_1 - T_2 \tan(k\ell_5)] [\cos \theta I_S(0, \theta) + I_S(L_1, \theta)F_1P_1(\pi - \theta)] + T_2 [I_S(0, \theta) - I_S(L_1, \theta)R(\pi - \theta, L_1)F_1] \quad (\text{A5})$$

$$W_0 = -G_0 / \cos(k\ell_4) - jT_1 \cos\theta I_0(0, \theta) + T_2 \left\{ \frac{I_0(\ell_5, \pi/2 - \theta)}{\cos(k\ell_5)} + I_0(0, \theta) - \left[1 + j \sin\theta \tan(k\ell_5) \right] I_0(0, \pi/2 - \theta) \right\} \quad (A6)$$

$$G_0 = - \left[I_0(\ell_1 + \ell_3 + \ell_4, \theta) + 2j \cos\theta (k\ell_1) \tan(k\ell_2) I_0(\ell_3 + \ell_4, \theta) \right] Q / \cos(k\ell_1) + \frac{\Omega}{\Psi} \frac{1 - R_2 F_2^2}{1 + F_2^2} \cos\theta I_0(\ell_4, \theta) + \left(\frac{1 - R_2 F_2^2}{1 + F_2^2} \cos\phi - 1 \right) I_s(0, \phi) e^{jk\ell_4 \cos\theta} + I_s(L_2, \phi) F_2 \left[R(\pi - \phi, L_2) + \frac{1 - R_2 F_2^2}{1 + F_2^2} P_2(\pi - \phi) \right] e^{jk\ell_4 \cos\theta} \quad (A7)$$

$$A_0 = -G_0 \sin(k\ell_4) + j \cos\theta I_0(0, \theta) + \frac{j\Psi}{\Omega} \left[\cos\theta I_s(0, \theta) + I_s(L_1, \theta) F_1 P_1(\pi - \theta) \right] \quad (A8)$$

$$P_i(\theta) = R(\theta, L_i) + \frac{1 - \cos\theta}{\Psi} \left\{ e^{jkL_i(1 - \cos\theta)} E_i \left[jkL_i(1 - \cos\theta) \right] + \frac{j}{kL_i(1 - \cos\theta)} \right\}, \quad i=1,2 \quad (A9)$$

$$F_i'^2 = F_i^2 P_i(\pi), \quad R_i = R(\pi, L_i), \quad F_i = F(L_i), \quad i=1,2 \quad (A10)$$

$$T_1 = T - \tan(k\ell_4) - \frac{\Omega}{j\Psi} \frac{1 - R_2 F_2^2}{1 + F_2^2} \quad (A11)$$

$$T_2 = \left[T_1 + \tan(k\ell_4) + \cot(k\ell_4) \right] \tan(k\ell_4) \quad (A12)$$

$$T_3 = \frac{1 - \tan(k\ell_3) [\tan(k\ell_1) + 2 \tan(k\ell_2)]}{1 - \tan(k\ell_3) \tan [k(\ell_4 + \ell_5)]} \quad (A13)$$

$$T_4 = \frac{1 - \tan(k\ell_3) [\tan(k\ell_1) + 2 \tan(k\ell_2)]}{[1 - \tan(k\ell_4) \tan(k\ell_5)] [1 - \tan(k\ell_3) \tan(k\ell_4 + k\ell_5)]} T_2 \quad (A14)$$

$$T = \cos(k\ell_3) [\tan(k\ell_1) + 2 \tan(k\ell_2) + \tan(k\ell_3)] Q \quad (A15)$$

$$Q = \left\{ \sin(k\ell_3) [\tan(k\ell_1) + 2 \tan(k\ell_2) - \cot(k\ell_3)] \right\}^{-1} \quad (A16)$$

These expressions were used to obtain numerical results for the induced wire currents. The expressions, albeit complicated, are explicit representations of the currents. They were coded on a microcomputer to obtain numerical results for the frequency variation of the wire current.

REFERENCES

1. L. Marin and K.S.H. Lee, "Response of the Dual-Wire (Counter-Poise) Antenna System on the E-4," Interaction Application Memos, Memo 20, June 1978.
2. L. Marin, "Current Induced on the VLF/LF Antenna Wires on the E-4 in the Resonance Region of the Aircraft," Interaction Application Memos, Memo 21, June 1978.
3. G. C. Lewis, Jr., L. Marin, "Transient Response of the Dual-Wire Antenna on the E-4," Interaction Application Memos, Memo 22, June 1978.
4. W. Curtis, "Trailing Wire Response Modeling," 1980 Summer Fulmen Meeting, Fulmen 5, May 13-15 1980.
5. W. A. Bereuther, "Calculation of the Parameters for the TACAMO Trailing-Wire Antenna Current Injection Test," 1980 Summer Fullmen Meeting, Fulmen 5, May 13-15 1980.
6. L. Marin, K.S.H. Lee, and T.K. Liu, "Response of the AS-1985/ARC-96 Trailing-Wire Antenna on the EC-135, Deliberate Aircraft Antenna Memos, Memo 19, Oct 75.
7. G. Bedrosian and L. Marin, "Transient Response of the Two HF Fixed-Wire Antennas on the EC-135, Deliberate Aircraft Antenna Memos, Memo 33, Feb 77,
8. L. C. Shen, T. T. Wu, and R. W.P. King, "A Simple Formula of Current in Dipole Antennas," IEEE Trans. Antennas & Propagation, Vol. AP-16, pp. 542-547, 1968.
9. L. C. Shen, "A Simple Theory of Receiving and Scattering Antennas," IEEE Trans. Antennas & Propagation, Vol. AP-18, pp. 112-114, 1970.
10. D.C. Chang, S. W. Lee, and L. Rispin, "A Simple Formula for Current on a Cylindrical Receiving Antenna," IEEE Trans. Antennas & Propagation, Vol. AP-26, pp. 683-690, 1978.
11. L. Marin, Carl E. Baum, and J. Philip Castillo, "A Simple Way of Simulating the EMP Effects of the VLF/LF Dual-Wire Antenna on the E-4," Miscellaneous Simulator Memos, Memo 14, November 1977.
12. M. Abramowitz and A. Stegun, Handbook of Mathematical Functions, U.S. Department of Commerce, AMS-55, November 1970.